

Elsevier Editorial System(tm) for Remote Sensing of Environment
Manuscript Draft

Manuscript Number:

Title: Comparison and Assessment of Coarse Resolution Land Cover Maps for Northern Eurasia

Article Type: Full length article

Keywords: Eurasia, Land cover, Global, Validation

Corresponding Author: Mr. Dirk Pflugmacher,

Corresponding Author's Institution: Oregon State University

First Author: Dirk Pflugmacher

Order of Authors: Dirk Pflugmacher; Olga N Krankina; Warren B Cohen; Mark A Friedl; Damien Sulla-Menashe; Robert E Kennedy; Peder Nelson; Tatiana Loboda; Tobias Kuemmerle; Egor Dyukarev; Vladimir Elsakov; Viacheslav I Kharuk

1 **Comparison and Assessment of Coarse Resolution Land Cover Maps**
2 **for Northern Eurasia**

3 Dirk Pflugmacher^{1*}, Olga Krankina¹, Warren Cohen², Mark Friedl³, Damien Sulla-
4 Menashe³, Robert Kennedy¹, Peder Nelson¹, Tatiana Loboda⁴, Tobias Kuemmerle⁵, Egor
5 Dyukarev⁶, Vladimir Elsakov⁷, Viacheslav I. Kharuk⁸,

6

7 ¹ Department of Forest Ecosystems and Society, Oregon State University, 321
8 Richardson Hall, Corvallis, OR 97331, USA

9 ² USDA Forest Service, Pacific Northwest Research Station, Forestry Sciences
10 Laboratory, 3200 SW Jefferson Way, Corvallis, OR 97331, USA

11 ³ Department of Geography and Environment, Boston University, 675 Commonwealth
12 Ave., 4th Floor, Boston, MA 02215, USA

13 ⁴ Department of Geography, University of Maryland, 2181 LeFrak Hall, College Park,
14 Maryland 20742, USA

15 ⁵ Forest and Wildlife Ecology, University of Wisconsin-Madison, 1630 Linden Drive,
16 Madison, WI 53706, USA

17 ⁶ Institute of Monitoring of Climatic and Ecological Systems, Tomsk, 634021, Russia,

18 ⁷ Institute of Biology, Komi Science Center, Russian Academy of Sciences,
19 Kommunisticheskaja st., 28, 167610 Syktyvkar, Russia

20 ⁸ V.N. Sukachev Institute of Forest, Krasnoyarsk, Russia

21

22 *corresponding author (email: dirk.pflugmacher@oregonstate.edu, phone: 1-541-750-

23 7287, fax: 1-541-737-1393)

24

25 Abstract

26 Information on land cover at global and continental scales is critical for addressing a
27 range of ecological and socioeconomic research questions. Coarse spatial resolution
28 sensors and algorithms for global land cover mapping have evolved rapidly in the last
29 decade, but efforts to evaluate map uncertainties have been limited, especially in remote
30 regions like Northern Eurasia. In this study we assessed four global land cover datasets:
31 GLC-2000, GLOBCOVER, and the MODIS Collection 4 and Collection 5 Land Cover
32 Products using Landsat-based reference maps at six test sites distributed across Northern
33 Eurasia. We developed a common legend based on dominant life form (Tree, Shrub, and
34 Herbaceous) to bridge differences in global map legends, and assessed map performance
35 at the pixel, pixel-block, test site, and continental scale. Accuracy assessment for pixel
36 and pixel-blocks was based on sub-pixel proportions of land cover to evaluate biases
37 associated with coarse resolution. Total pixel-level agreement between global maps and
38 test sites ranged from 0.67-0.74, and kappa ranged from 0.41-0.52 indicating fair to
39 moderate agreement. The representation of tree-dominated classes was most accurate,
40 while differences in the classification of non-tree classes accounted for most of the
41 disagreement among global datasets. Tree-dominated classes tended to be over-
42 represented at test sites as a result of the coarse spatial resolution. Accuracy estimates for
43 pure (coarse-resolution) pixels and sampling units between 2 x 2 and 5 x 5 pixel blocks
44 were 7-45% higher than pixel-level results, indicating that accuracy estimates from global
45 maps based on homogeneous or dominant land cover types are likely too optimistic. If
46 global maps are compared at our test sites using pixel-blocks of equal area, e.g. 3 x 3 km

47 then the overall agreement of GLOBCOVER (0.80) is similar to that of GLC-2000
48 (0.81), and MODIS V5 (0.81), and is higher than that of MODIS V4 (0.75). Because the
49 choice of evaluation criteria and sampling unit can lead to significantly different
50 estimates of map accuracy, a better understanding of the effect of accuracy measure
51 selection is needed. Knowledge of biases in different global products is important for
52 their applications in global assessments and informing policy decisions.

53 1 Introduction

54 Information on land cover at global and continental scales is critical for addressing a
55 range of important science questions from effects of vegetation on the carbon cycle,
56 surface energy, and water balance, to understanding socioeconomic causes and
57 consequences of land-use and land-cover change. The need for accurate land-cover
58 information is particularly acute in Northern Eurasia. The area is a locus for climate
59 change, and there is mounting evidence of significant recent changes in vegetation
60 distribution, growing season duration, and patterns of snow cover and permafrost (i.e.
61 Chapin et al. 2005; Groisman et al. 2009). The region also has unique, but often poorly
62 characterized features, including vast expanses of larch (*Larix* spp.) forests, permafrost,
63 wetlands, widespread disturbances (fire, harvest, pollution damage, insect damage), and
64 drastic changes in land use following profound region-wide socioeconomic changes in
65 the 1990s (e.g. Forbes et al. 2004; Kuemmerle et al. 2008; Kuemmerle et al. 2009).

66 Since the mid 1990s substantial advances have been made towards the development of
67 global vegetation and land cover datasets from moderate resolution satellite sensors. The
68 first satellite-based global land cover maps were produced with data from the advanced
69 high-resolution radiometer (AVHRR) (DeFries and Townshend 1994; Hansen et al. 2000;
70 Loveland et al. 2000). In 1998 and 1999, AVHRR was followed by VEGETATION-1
71 onboard the fourth Satellite Pour l'Observation de la Terre (SPOT) and the Moderate
72 Resolution Imaging Spectroradiometer (MODIS), which started the concurrent
73 development of two additional global land cover products: GLC-2000 (Bartholome and
74 Belward 2005) and the MODIS Global Land Cover Product (Friedl et al. 2002). More

75 recently, two new global land cover datasets have been released: GLOBCOVER derived
76 from Medium Resolution Imaging Spectrometer (MERIS) data (Arino et al. 2008) and
77 the MODIS C5 Land Cover Product (Friedl et al. 2010). The most important change in
78 the evolution of these datasets is the increase in spatial resolution from ~1km (MODIS
79 C4 and GLC-2000) to ~500m (MODIS C5) and ~300m (GLOBCOVER). The finer
80 resolution of these maps is expected to improve global land cover characterization.

81 The availability of multiple relatively similar land cover data sets provides the user
82 community with a choice, but it is not clear for most users which map suits their
83 particular application best (Herold et al. 2008; Jung et al. 2006). Ultimately, the selection
84 is often based on map legends rather than accuracy, in part because it is difficult to
85 ascertain which map is the most accurate. Map developers commonly report overall
86 estimates of map accuracy, however, because of methodological differences these
87 measures cannot be directly compared. For example, the reported classification accuracy
88 for MODIS V5 (75%, Friedl et al. 2010) is 8% higher than the reported accuracy for
89 GLOBCOVER (67%, Bicheron et al. 2008), but the significance of this difference is
90 uncertain.

91 While users often rely on overall measures of map accuracy to evaluate the quality of
92 maps, map errors are rarely equally distributed (Strahler et al. 2006). Therefore, two
93 maps can have the same overall accuracy, but show a different spatial distribution of
94 error. In this case, the choice of map would depend on user interest in a particular region
95 of the map and will need to be considered in interpreting results of spatial modeling.
96 Studies that compared global land cover maps found significant variability in class

97 agreement between biomes (Fritz and See 2008; Giri et al. 2005; Herold et al. 2008).
98 Disagreement is largest for spectrally similar land cover types (e.g. mixed versus pure
99 broadleaf and conifer forests) and spatially heterogeneous land cover. Geographic areas
100 affected most by the disagreement among maps are the transition zones between major
101 biome types and areas more profoundly influenced by human land-use activities. In
102 Northern Eurasia these are regions that have historically been influenced by, and
103 potentially will be most vulnerable to, socioeconomic and climate changes.

104 Despite the importance of Northern Eurasia for global change research, global maps have
105 not been rigorously tested in this region. Frey and Smith (2007) compared field
106 observations in Western Siberia with two land cover and two wetland databases.

107 Agreement between the field data and the two analyzed land cover data sets, the AVHRR
108 Global Land Cover Characterization Database and the MODIS C3 Land Cover Product,
109 was 22% and 11%, respectively. Other comparison studies have focused only on
110 wetlands (Krankina et al. 2008; Pflugmacher et al. 2007).

111 Cross comparisons between global land cover maps help identify areas of potential high
112 map uncertainty (Herold et al. 2008; See and Fritz 2006), but independent validation
113 studies are needed to reveal the sources of disagreement and provide local and regional
114 scale estimates of classification accuracy. There are several challenges associated with
115 this task:

116 - The collection of reference data is costly for large areas, particularly for remote
117 regions such as Northern Eurasia. Consequently, it is crucial to design and
118 implement validation methods that are not tailored to a single map product, i.e. a

119 single classification system and spatial resolution, but that can accommodate a
120 range of current and potentially future land cover maps.

121 - Reference data is often collected at high spatial resolution and needs to be
122 aggregated to the resolution of the coarse-scale map. The process of aggregation,
123 however, can introduce biases towards dominant land cover types ("low
124 resolution bias", Boschetti et al. 2004; Latifovic and Olthof 2004).

125 - Accuracy estimates depend on the choice of sampling unit (e.g. pixels or pixel-
126 blocks), which often differ from the spatial unit of the map (Foody 2002).
127 Commonly, a single analysis unit is used in assessments although land cover
128 maps are used on a variety of spatial scales (including the pixel-scale).

129 - Maps differ with respect to class definitions and thematic detail they provide. This
130 affects estimates of overall map accuracy (Latifovic and Olthof 2004), and
131 therefore makes cross-comparison of accuracy estimates difficult.

132 The objective of this study was to evaluate accuracy measures and procedures for
133 validating four major global land cover datasets over the region of Northern Eurasia
134 using maps created from higher resolution satellite data (Landsat). This study is part of a
135 broader effort to validate and improve land cover and land-cover change products for
136 Northern Eurasia using a network of local test sites distributed throughout the region
137 (<http://www.fsl.orst.edu/nelda>).

138 2 Methods

139 For the purpose of this analysis we defined the region of Northern Eurasia to extend from
140 42°–74° N latitude; and we included Scandinavia, the Baltic countries, Belarus, Moldova
141 and the Ukraine (Figure 1). Reference sites were selected to cover a range of geographic
142 and climatic gradients in locations where high quality reference data and local expertise
143 were available. Our reference data consists of land cover maps for each site compiled
144 from Landsat scenes and a combination of ground data and expert knowledge. Using
145 Landsat-based maps allowed for detailed exploration of the distribution of land cover and
146 error structure associated with selected landscape types. A similar approach has been
147 used to validate MODIS Land Cover maps for selected biome types in North and South
148 America (Cohen et al. 2006; Cohen et al. 2003; Latifovic and Olthof 2004). While
149 random probability sampling is more desirable (Strahler et al. 2006), validation studies
150 are often constrained by availability of reference data. Opportunistic selection of
151 validation sites precludes a probability-based statistical assessment of the global maps
152 overall, but permits different measures of map accuracy to be examined across a wide
153 range of conditions within Northern Eurasia.

154 2.1 Global land cover data sources

155 The GLC-2000 effort was lead by the Joint Research Center of the European
156 Commission in partnership with more than 30 institutions (Bartholome and Belward
157 2005). The GLC-2000 map is based on Satellite Pour l'Observation de la Terre (SPOT)
158 VEGETATION data acquired daily between November 1999 and December 2000. The
159 map uses a 22-class legend based on UN FAO's hierarchical Land Cover Classification

160 System (LCCS, DiGregorio 2005). We downloaded the global data set (v1.1) from
161 (<http://www-gvm.jrc.it/glc2000/>; last accessed 20 January 2008) in geographic
162 coordinates, and projected it to an equal area projection (Lambert Azimuthal EA).

163 GLOBCOVER is the successor to GLC-2000, and as such also builds on an international
164 network of partners. GLOBCOVER was developed using an annual mosaic of Envisat's
165 Medium Resolution Imaging Spectrometer (MERIS) data from December 2004 to June
166 2006. With 300 m spatial resolution, GLOBCOVER represents the highest spatial
167 resolution global land cover dataset currently available. The map distinguishes between
168 22 classes that are compatible with the Land Cover Classification System (LCCS). We
169 downloaded GLOBCOVER v2.2 from the European Space Agency GLOBCOVER
170 Project (<http://ionial.esrin.esa.int>, last accessed 12 December 2008).

171 The MODIS Land Cover Product is developed by scientists from Boston University for
172 NASA's Earth Observing System (EOS) MODIS land science team (Friedl et al. 2002).

173 The MODIS Land Cover Product provides global land cover in five different
174 classifications, and is produced for each year since 2001. The MODIS land science team
175 periodically reprocesses MODIS reflectance and data products, including the yearly
176 MODIS Land Cover Product. For this study we analyzed MODIS Land Cover Collection
177 4 data from 2001 and Collection 5 data from 2005 using the classification of the
178 International Geosphere-Biosphere Programme (IGBP) classification system, hereafter
179 referred to as MODIS V4 and MODIS V5, respectively. We obtained the data from the
180 NASA Warehouse Inventory Search Tool (<https://wist.echo.nasa.gov>, last accessed 25
181 January 2010).

182 2.2 Differences between global land cover classifications

183 The global land cover classifications analyzed in this study are generally similar, but
184 there are differences between maps that make a direct and uniform comparison
185 challenging (Table 1). For example GLC-2000 differentiates between evergreen and
186 deciduous shrub types, whereas MODIS IGBP does not distinguish between shrub leaf
187 types, but does distinguish between open and closed shrub cover. Further, GLC-2000 and
188 GLOBCOVER distinguish between non-vegetated, bare land cover and sparse vegetation
189 with less than 10-20% and less than 15% vegetation cover, respectively. In comparison,
190 MODIS IGBP combines these land cover types into a single class: barren and sparsely
191 vegetated areas with less than 10% vegetation or snow cover. Maps also show various
192 degrees of thematic detail within tree life form classes. Generally, tree life form types are
193 characterized by leaf type (needleleaf, broadleaf, and mixed) and seasonal phenology
194 (evergreen and deciduous). However, each map contains classes that cannot be
195 unambiguously assigned to either of the two, e.g. the “Burnt Tree Cover”, “Regularly
196 Flooded Tree Cover”, and “Mosaic Tree Cover” classes in GLC-2000, the “Open
197 Needleleaved Deciduous or Evergreen Forest” class in GLOBCOVER, and the open tree
198 vegetation cover classes in MODIS IGBP (“Woody Savannas” and “Savannas”). The
199 common denominator to each of the global classification systems examined here are the
200 dominant life form types, e.g. tree, shrub, herbaceous vegetation and non-vegetated land
201 cover such as barren, snow and ice, and water.

202 To minimize ambiguities in comparison of accuracy statistics among global land cover
203 datasets, map legends need to be converted to a common classification. For this paper, we
204 generalized map legends to six classes on the basis of the dominant life form types (LFT)

205 in each map (Table 1). Croplands were labeled as herbaceous vegetation and classes that
206 include mixtures of LFT types were labeled as “mosaic”. This level of generalization
207 avoids most of the ambiguities described above, albeit at the cost of thematic detail. An
208 alternative approach to bridging the differences among legends relies on “fuzzy logic”
209 (See and Fritz 2006) in contrast to “crisp logic” chosen for this study. We opted for crisp
210 comparison in an effort to maintain objectivity by avoiding judging the severity of class
211 disagreement.

212 2.3 Test sites

213 To assess the coarse resolution maps we selected six test sites across wide latitudinal,
214 longitudinal, and climatic gradients of Northern Eurasia (Table 2, Fig. 1). Mean annual
215 temperature ranges from -5 °C at the Komi site to +6 °C at the Carpathian site and
216 precipitation ranges from <400 mm per year in Chita to about 1000 mm in the
217 Carpathians. While all sites have mild summers, the average winter temperature declines
218 from west to east as the climate becomes increasingly continental. The terrain is flat at
219 the St. Petersburg, Komi and Vasyugan site and mountainous with significant elevation
220 gradients at the remaining three sites.

221 All sites are located within the forest belt that stretches across Northern Eurasia and
222 vegetation cover in all sites includes a significant proportion of forest (tree-dominated
223 land cover). Shrub cover is present in all sites as well, but its role tends to be small. The
224 sites represent different ecoregions including temperate forest (Carpathians), southern
225 taiga or boreal forest (St. Petersburg and Vasyugan), northern taiga (Komi), and montane
226 boreal (Priangarie and Chita) (Alexeyev and Birdsey 1998). The sites also reflect the

227 diversity of vegetation disturbance regimes in Northern Eurasia, including forest fires
228 (Chita), insect outbreaks (Priangarie), timber harvest (Carpathians and St. Petersburg),
229 and changes in agricultural land use (all sites except Komi). Wetlands occupy large areas
230 at three test sites (St. Petersburg, Komi, and Vasyugan). Excessive moisture at these sites
231 leads to accumulation of peat, reduced density of tree cover and greater shrubs and
232 herbaceous vegetation cover.

233 Detailed land cover maps for each test site were developed based on Landsat imagery
234 combined with local expert knowledge and ground data. Results of several completed and
235 ongoing projects that mapped land cover and examined various types of land-cover, land-
236 use change, and vegetation disturbance were also used (e.g., Heikkinen et al. 2004;
237 Kharuk et al. 2004; Kharuk et al. 2003; Krankina et al. 2004a; Krankina et al. 2004b;
238 Kuemmerle et al. 2007; Kuemmerle et al. 2008). The Landsat classification approaches
239 varied by site and included supervised (e.g. decision trees) and unsupervised
240 classifications. All site legends followed the Land Cover Classification System (LCCS,
241 Di Gregorio 2005) and included between 11 and 17 classes. These were recoded into the
242 following dominant life form classes: tree, shrub, herbaceous vegetation, and barren or
243 sparse vegetation (Table 3). The LCCS classification defines “tree dominated” cover as
244 land with greater than 15% tree cover, where trees are any woody vegetation taller than 5
245 m or trees taller than 3 m. Similarly, shrub and herbaceous dominated vegetation types
246 have a minimum of 15% plant cover, respectively. The dominant life form is defined
247 hierarchically by the height of the canopy layer, which ranges from trees to shrubs to
248 herbaceous plants. Lands with less than 15% vegetation cover are labeled as “bare land
249 and sparse vegetation”.

250 Map accuracy at test sites was assessed using forest inventory data and ground
251 observations from research projects. Where ground observations proved insufficient,
252 additional reference data were collected through manual interpretation of aerial photos
253 and high-resolution imagery in Google Earth. The overall accuracy of Landsat-derived
254 maps for dominant life forms exceeded 92% for Carpathians, St. Petersburg, Vasyugan,
255 and Priangarie sites; it was somewhat lower for Chita and Komi sites (87% and 80%,
256 respectively) (Table 3). For the purpose of this study the Landsat-based classifications are
257 considered “ground truth”.

258 2.4 Comparison and assessment of global maps

259 To assess the accuracy of the four global maps we explored the distribution of global land
260 cover at the regional (Northern Eurasia), local (test sites), and pixel/pixel-block scale
261 (within test sites). Comparisons of total map and reference class proportions are effective
262 to assess global land cover maps at the test site scale (Cohen et al. 2006), but a more
263 rigorous approach was required to evaluate the spatial agreement for coarse resolution
264 pixels and pixel-blocks. Error or confusion matrices are commonly used for reporting the
265 accuracy of thematic maps (Foody 2002). Several measures can be derived from these
266 matrices such as the error of omission (exclusion) and commission (inclusion), and
267 overall agreement and kappa (Cohen 1960). Like overall agreement, kappa ranges from 0
268 to 1, but its interpretation is less transparent. In general, kappa estimates between 0.6-0.8
269 are interpreted as good to very good, and between 0.4-0.6 as fair to moderate
270 (Czaplewski 1994).

271 Reference data for validating global map products are often acquired at higher spatial
272 resolution, but conventional error matrices require the reference data to match the spatial
273 resolution of the map to be validated. As a consequence, when maps with differing spatial
274 resolutions are compared, the map with the higher spatial resolution is often aggregated
275 to the coarser resolution by assigning the dominant class to the aggregated pixel
276 (Stehman and Czaplewski 1998; Turner et al. 2000). The disadvantage of this approach is
277 that it assumes a level of homogeneity in the landscape, which rarely is the case, and as a
278 result sub-dominant and rare classes are often under-represented. The extent of this low
279 resolution bias depends on the patchiness of land cover. For example, in a study that
280 assessed the representation of wetlands in global and continental land cover maps in the
281 St. Petersburg region, we found that 50% of the wetland area would be omitted if 30 m
282 reference pixels were aggregated to 1 km pixels using the dominant class rule (Krankina
283 et al. 2008).

284 The sub-fractional error matrix introduced by Latifovic and Olthof (2004) provides a
285 method to summarize reference class proportions within coarse map pixels and therefore
286 avoids spatial aggregation of the reference data. The sub-fractional error matrix is
287 populated by counting the number of pixels of a reference class within a coarser
288 resolution pixel (Figure 2a). Thus, instead of labeling a coarse resolution pixel either
289 100% correct or 100% incorrect, the “correctness” of that pixel is rated on a continuous
290 scale based on the pixel fraction occupied by the “correct” reference class. Standard
291 accuracy measures calculated from conventional error matrices can also be computed
292 from the sub-fractional error matrices. For example, omission error is the fraction of
293 reference pixels that occupy coarse resolution pixels of other classes. Similarly,

294 commission error is the total sub-pixel fraction of coarse resolution pixels occupied by
295 reference pixels of other classes. Because coarse resolution pixels usually contain a
296 mixture of cover classes, total agreement scores obtained by this approach are generally
297 less than 1 even if the classification were perfect.

298 Classification accuracy can also be expected to decrease with increased fine-scale
299 heterogeneity in land cover types (Herold et al. 2008). To measure map accuracy
300 independent of coarse resolution bias and landscape heterogeneity, we calculated
301 accuracy statistics for “pure” pixels. Pure pixels contain at least 95% of a single land
302 cover class in the reference data.

303 Mosaic classes of global land cover classifications contain mixtures of vegetation types,
304 e.g. croplands, forests, shrub land, and grasslands that only occur at the coarse resolution
305 scale. This is problematic in accuracy assessment, because it is not clear when a pixel
306 should be labeled as mosaic and when it should be labeled according to the dominant
307 vegetation type. For example, an area with 30% tree cover could be classified either as
308 mosaic or forest. To account for this ambiguity we assume that mosaic pixels can contain
309 any combination of tree, shrub and herbaceous vegetation types. Thus, total agreement
310 for mosaic pixels was determined from the combined area of tree, shrub and herbaceous
311 reference pixels. Similarly, when we calculated omission errors for these three classes,
312 the area mapped as mosaic was added to tree, shrub, and herbaceous LFT, respectively,
313 effectively decreasing the omission error. This approach yields a conservative assessment
314 of map error as it reduces the uncertainty resulting from mosaics, but it potentially

315 inflates the map accuracy measures in proportion to the area classified by global maps as
316 mosaic or mixed vegetation.

317 Errors in spatial registration of individual coarse-resolution pixels also introduce
318 uncertainty when linking a coarse-resolution pixel to a set of fine resolution pixels on a
319 reference map. To account for potential misregistration errors, we estimated map
320 accuracies for different sizes of sampling units: ranging from individual coarse resolution
321 pixels to blocks ranging in size from 2 x 2 to 10 x 10 coarse resolution pixels. The sub-
322 fractional error method has previously only been used with sampling units of individual
323 pixels (Latifovic and Olthof 2004). However, the method can also be applied to pixel
324 blocks. For the purpose of demonstration it is convenient to describe the fractional error
325 matrix using terminology from set theory, where the set boundaries are defined by the
326 sampling unit and the set elements are the map pixels (Figure 2b). Because we are
327 interested in sub-pixel fractions of land cover, the coarse map must be resampled to the
328 spatial resolution of the reference data. The class agreement of a reference sample X and
329 a global map sample X' is then the intersection between the two sets, and the overall class
330 agreement is the sum of intersections across all samples:

331
$$Y_{i,i} = \sum_{m=1}^M \sum_{n=1}^N X_{m,n} \cap X'_{m,n} \quad \text{Eq. 1)}$$

332 where i denotes the row and column (diagonal) of error matrix Y , and m and n denote the
333 row and column of the accuracy samples, respectively. Note that because the sampling
334 unit is greater than the map unit, non-diagonal elements do not have a unique solution.

335 The calculation of agreement, omission and commission for pixel blocks is similar to that
336 of individual pixels.

337 3 Results

338 3.1 Comparison of land cover distributions for Northern Eurasia

339 There are significant differences among global maps with respect to spatial distribution
340 and relative frequency of vegetation types in Northern Eurasia. Estimates of the tree
341 dominated land area are relatively similar for the entire region, ranging from 35%
342 (MODIS V4) to 42% (GLC-2000) (Figure 3). However, differences in tree cover are not
343 equally distributed but concentrated mainly in northern Siberia and the Far East. For
344 example, tree cover in GLC-2000 and GLOBCOVER is significantly higher in the
345 transition zone between boreal forest and shrub tundra compared to MODIS V4 and
346 MODIS V5 (Figure 4).

347 MODIS maps a significant proportion of the northern taiga and the tundra as shrub
348 dominated vegetation. Based on MODIS V4 and V5, shrub land cover types make up
349 about one quarter of the entire Northern Eurasia region (27% and 21%, respectively).
350 This is about three times the total shrub dominated land area mapped by GLC-2000 (7%).
351 Interestingly, GLOBCOVER classifies less than 0.1% of Northern Eurasia as shrub lands,
352 but maps a significantly greater proportion of the region as sparse vegetation and barren
353 land (31%) when compared to GLC-2000 (23%), and MODIS V4 (6%) and V5 (4%).
354 The difference is most pronounced in the taiga-tundra ecotone and in the transition from
355 steppe/grasslands to non-vegetated areas in the south, where herbaceous vegetation cover

356 is significantly greater with MODIS. However, GLOBCOCOVER maps about 22% of the
357 region as vegetation mosaics, which partly explains its low proportion of herbaceous and
358 shrub dominated vegetation classes. The proportion of mosaic pixels is significantly
359 lower in GLC-2000 (9%), MODIS V4 (1%), and MODIS V5 (6%).

360 3.2 Comparison of global land cover at test sites

361 3.2.1 Distribution of global land cover at test sites

362 Comparison of the four global land cover datasets with the Landsat-based reference maps
363 (Figure 5) revealed general patterns of agreement and disagreement at the site level. To
364 quantify the representation of global land cover at this scale, we compared the relative
365 proportions of dominant life form types (LFT) at each site without regard of their within-
366 site spatial distribution (Figure 6a). We found the percentage of coarse resolution pixels
367 in the tree class matches most closely the percentage of reference pixels across all global
368 maps. GLOBCOVER shows the highest overall agreement in this class (88%), followed
369 by GLC-2000 (82%), MODIS V5 (80%), and MODIS V4 (78%). There is a general
370 tendency in all four coarse resolution maps to overestimate the tree class by an average of
371 10-20% (Figure 6a). The pattern of under-reporting smaller classes does not improve on
372 maps with finer resolution (GLOBCOVER and MODIS V5). The same analysis
373 performed on coarse resolution pure pixels with uniform land cover (Figure 6b) shows a
374 much improved agreement in total tree dominated area and other LFT classes for all
375 global maps, although the improvement for non-tree classes is notably smaller for
376 GLOBCOVER.

377 Differences in LFT class proportions between global maps and reference data are largest
378 where tree cover is sparse. At Komi, GLC-2000 and GLOBCOVER overestimate tree
379 cover by 30% and 26%, respectively, whereas MODIS V4 under-represents this class by
380 40%. The low percentage of tree cover in V4 is accompanied by a significantly higher
381 proportion of shrub cover; 2.6 times higher than the reference data. In MODIS V5,
382 classification of tree vegetation significantly improved and is more consistent with GLC-
383 2000 and GLOBCOVER. Conversely, GLOBCOVER significantly overestimates
384 barren/sparse vegetation all test sites, but shows the best agreement for inland water
385 bodies.

386 3.2.2 Pixel-based agreement of global maps

387 Total agreement for pixel-level comparisons ranges from 0.34 at the Komi site based on
388 GLOBCOVER to 0.87 at the Carpathian site based on MODIS V5 (Table 4). Mean total
389 agreement from all global maps ranges from 0.46 ± 0.09 at Komi to 0.84 ± 0.02 at
390 Priangarie. For all sites combined, total agreement for MODIS V4 and V5 was 0.67 and
391 0.74, respectively; and for GLOBCOVER and GLC-2000 total agreement was 0.70 and
392 0.73, respectively. MODIS V5 performed better than MODIS V4 on all test sites with the
393 exception of Chita. The lower agreement at Chita may be attributable to widespread
394 forest fires that burned about 17% of the total site area in 2002-2003, most of it tree-
395 dominated. The time of these disturbances falls in-between the Landsat and MODIS V5
396 data acquisitions in 2000 and 2005, respectively. The time difference to the reference
397 maps is the same as that for GLOBCOVER, but larger compared to GLC-2000 and
398 MODIS V4. However, on average the disturbance rates do not exceed 0.1-0.2% per year
399 over large areas. Thus, we expect the effect of differences in the data acquisition dates to

400 be small on all sites with the exception of Chita. Chance corrected agreement at the pixel
401 scale is fair to moderate for all maps ($Kappa = 0.41-0.52$).

402 The sub-pixel fractional error matrices for dominant life form types reveal more detailed
403 patterns of class confusions across test sites (Table 5). Class errors are lowest for tree
404 vegetation with omission errors (OE) between 0.05 (GLC-2000 and GLOBCOVER),
405 0.08 (MODIS V5) and 0.13 (MODIS V4), and commission errors between 0.2
406 (GLOBCOVER and MODIS V5) and 0.24 (GLC-2000). For individual test sites
407 omission of tree land cover is less than 0.2 except at Chita (evidently due to fire, MODIS
408 V5, $OE=0.28$) and Komi (MODIS V4, $OE=0.59$). Because these error estimates
409 correspond to sub-pixel proportions of land cover, omission and commission errors
410 describe the approximate boundaries of the mapped classes. For example, a 0.05
411 omission error indicates an average tree cover in non-tree pixels of 5%. Likewise, a
412 commission error of 0.2 represents the mean fraction of non-tree cover included in coarse
413 resolution tree pixels. Because global maps typically define a minimum tree cover
414 threshold for tree dominated classes between 10-20%, it is reasonable to expect an
415 average omission of up to 0.1-0.2, depending on class definition. Tree cover in this study
416 is defined at the Landsat resolution with a minimum cover threshold of 15%.

417 Shrub cover tends to be under-represented with overall omission rates between 0.54
418 (MODIS V5) and 0.82 (GLOBCOVER). However, only 40%-52% of the omitted shrub
419 cover can be attributed to coarse resolution tree pixels. If we exclude shrub cover
420 associated with these pixels, we obtain omission errors of 0.14 (MODIS V5), 0.15 (GLC-
421 2000), 0.16 (MODIS V5) and 0.39 (GLOBCOVER). Examination of the error matrices in

422 Table 5 reveals, that over 90% of the omitted shrub cover is mapped as barren by
423 GLOBCOVER, and herbaceous by GLC-2000 and MODIS. Similarly, about 50% of the
424 omitted herbaceous cover is mapped as tree or barren, respectively, in GLOBCOVER.
425 This indicates that GLOBCOVER underestimates shrub cover and herbaceous cover
426 while overestimating barren/sparse vegetation. Conversely, MODIS maps large areas of
427 herbaceous tundra as open shrub land.

428 3.2.3 Global map agreement for homogenous land cover

429 To quantify the effect of landscape homogeneity on map accuracy we performed a
430 separate accuracy assessment for pure pixels. There is a clear relationship between the
431 number of pure pixels and map agreement between test sites (Figure 7). The Priangarie
432 site with the highest overall agreement also has the highest percentage of pure pixels
433 (50%-67%), whereas Komi site with the lowest map agreement shows the lowest
434 percentage of pure pixels (3%-13%). As expected, maps with higher spatial resolution
435 exhibit a greater number of pure pixels. The spatial resolution of GLOBCOVER is much
436 higher than that of GLC-2000 and MODIS V4, and its percentage of pure pixels is about
437 twice as high as these two maps at St. Petersburg, Carpathian, and Vasyugan, and 4.5 and
438 1.3 times as high at Komi and Priangarie, respectively. However, there is no clear
439 relationship between number of pure pixels and total agreement within test sites and
440 between maps indicating that factors other than spatial resolution also affected map
441 accuracy.

442 The agreement of global maps is nearly perfect if only pure pixels are considered (Table
443 4). Except at the Komi site, total agreement for dominant life form types exceeds 0.9.

444 Kappa also indicates good and perfect agreement for pure pixels. Total agreement
445 increases for pure pixels compared with all-pixel results between 0.09 and 0.45, with a
446 higher increase at sites with heterogeneous land cover (e.g. 0.31-0.45 at Komi) and lower
447 increase at more homogeneous sites (e.g. 0.09-0.17 at Priangarie). Further, the effect is
448 greater for the 1-km resolution maps GLC-2000 (mean = $0.23 \pm$ standard deviation =
449 0.06) and MODIS V4 (0.27 ± 0.10) than for GLOBCOVER (0.18 ± 0.08) and MODIS
450 V5 (0.19 ± 0.08).

451 3.2.4 Agreement of global maps for different sampling units

452 In previous sections we assessed the accuracy of global maps by examining the
453 agreement of individual coarse resolution pixels with reference data. To explore the
454 effect of the sampling unit on map agreement, we increased the size of the unit from a
455 single pixel to blocks of pixels (e.g. 2 x 2, 3 x 3 coarse resolution pixels).

456 On average across sites, total agreement between global maps and reference data
457 increases between 0.089 ± 0.002 (MODIS V5) and 0.136 ± 0.002 (GLC-2000) for pixel-
458 blocks of up to 10 x 10 pixels relative to the single pixel case (Figure 8). The effect is
459 slightly larger for the coarser GLC-2000 and MODIS V4. Increase in agreement is
460 strongest for 2 x 2 pixels blocks, i.e. 0.062 ± 0.037 for GLC-2000, 0.040 ± 0.015 for
461 GLOBCOVER, 0.056 ± 0.013 for MODIS V4, and 0.037 ± 0.011 . The rate of
462 improvement diminishes rapidly to about $10\% \pm 2\%$ of the agreement estimate when
463 block sizes of 5 x 5 pixels are reached.

464 4 Discussion

465 This study presents an approach to assess global land cover maps consistently for the
466 region of Northern Eurasia, and to explore the effect of sampling unit, reference class
467 assignment and landscape characteristics on accuracy statistics. Our results show that
468 methodology and choice of sampling unit significantly influence accuracy estimates,
469 which indicates that reported global map statistics should be compared with caution. All
470 analyzed maps showed similar overall agreement with Landsat-based reference data.
471 However, results of accuracy assessments at test sites and regional statistics for Northern
472 Eurasia indicate that similarities in map agreements are mostly due to similar
473 representations of tree dominated land cover. Though slightly overestimated, tree
474 dominated vegetation is the most accurate land cover class in all maps, whereas there are
475 significant differences in the representation of non-tree land cover classes.

476 Our results indicate that global map accuracies for Northern Eurasia are likely lower than
477 the reported global estimates from map developers. While methodological differences
478 make a comparison difficult, our accuracy estimates based on six test sites (Table 4) are
479 generally in line with the published global estimates for the examined maps (Bicheron et
480 al. 2008; Friedl et al. 2002; Friedl et al. 2010; Mayaux et al. 2006). However, given that
481 our analysis was based on a simplified 6-class legend, we expect that comparisons based
482 on the full classification of these maps produce lower agreements for Northern Eurasia.
483 Further, our analysis was not limited to homogenous areas or dominant land cover classes
484 as is often practice in global map validation.

485 Total agreement between global land cover and reference data is similar among maps
486 (0.67-0.74), although MODIS V5 and GLC-2000 produce slightly better results than
487 MODIS V4 and GLOBCOVER. Pixel-level map accuracy increases by 7% from MODIS
488 V4 to MODIS V5, and decreases by 3% between GLC-2000 and GLOBCOVER.
489 However, when sampling units of equal area are compared, e.g. 3 x 3 km then total
490 agreement of GLOBCOVER (0.80) is similar to that of GLC-2000 (0.81), and MODIS
491 V5 (0.81), and is higher than that of MODIS V4 (0.75).

492 Tree dominated land cover is the most accurately mapped class in all global datasets. The
493 accuracies for our six test sites are within the range that can be expected from thematic
494 coarse resolution maps. Commission errors of 20% for tree dominated classes are
495 common and can be explained by the coarse spatial resolution. The high agreement for
496 pure pixels corroborates this.

497 Map disagreements are concentrated in areas with sparse tree cover and mixtures of
498 herbaceous and shrub cover, predominantly found in the taiga-tundra ecotone. The
499 hierarchical nature of land cover classifications, which define vegetation types based on
500 the order of presence of trees, shrub and then herbaceous vegetation and not the land
501 cover type that occupies the majority of the area, may increase the likelihood of class
502 confusion in transition zones of vegetation types. For example, a pixel that is comprised
503 to 20% of shrub, 40% herbaceous and 40% barren is defined as (open) shrub land, but the
504 dominance of herbaceous vegetation and barren will increase the probability that that
505 pixel is misclassified as either of the two more dominant classes. Hierarchical
506 classifications that 'weight' vegetation types differently according to their 'ecological

507 value' are commonsense, but nevertheless it imposes additional requirements on thematic
508 coarse resolution maps to accurately represent sup-pixel land cover proportions.

509 Approaches that directly estimate sub-pixel proportions of land cover types might
510 provide a meaningful alternative for this task (Hansen et al. 2002; Hansen et al. 2005).

511 Subdominant and rare classes that exist largely at the sub-pixel scale are difficult to
512 resolve with thematic coarse resolution maps. Despite their spectrally distinct signature,
513 inland water bodies show omission errors between 50-70%. Representation of
514 subdominant and rare classes improved for pure pixels compared to all pixels (Figure
515 6a,b), although the improvement was less significant for GLOBCOVER. While the finer
516 resolution of GLOBCOVER could be expected to improve the accuracy of small classes,
517 water was the only class more accurately mapped by GLOBCOVER. It appears with finer
518 resolution other sources of error including pixel registration, become more significant. In
519 this context, it is important to note that the GLC-2000 and GLOBCOVER maps were
520 only available in a geographic coordinate system and had to be reprojected to an equal
521 area projection prior to analysis. Thus, registration errors may have been more significant
522 for these two maps.

523 We found overall accuracies increased by 8-12% for blocks of 5 x 5 pixels compared to
524 per-pixel comparisons, and that block sizes larger than 5 x 5 did not increase the
525 accuracies significantly (Figure 8, 9). While map accuracies are usually reported for a
526 single spatial analysis unit, maps are often used at multiple spatial scales (e.g. pixels,
527 polygons, pixel blocks). Because classification errors cannot be assumed to be the same
528 across different spatial scales, this introduces additional uncertainty for map users.

529 Furthermore, errors unrelated to map classification such as spatial misregistration and
530 convolution of the sensor signal with neighboring pixels can significantly influence the
531 underlying remote sensing data (Townshend et al. 2000), which suggests that
532 measurements of land cover properties are more robust at spatial resolutions coarser than
533 the individual pixel. In fact, reported accuracy statistics of global maps are often obtained
534 from sampling units larger than current coarse resolution map products (Stehman and
535 Czaplewski 1998), and only homogeneous or dominant land cover types are generally
536 sampled (Bicheron et al. 2008; Friedl et al. 2002; Friedl et al. 2010; Mayaux et al. 2006).
537 Because pixels are the basic mapping units of most global land cover data, users may not
538 always be aware of the uncertainties associated with using these maps at the pixel scale.
539 Our analysis of the effect of sampling unit on accuracy measures (Figure 8, 9) suggests
540 that blocks of 5 x 5 pixels are a good compromise between increased overall agreement
541 and decreased spatial detail.

542 To compare accuracy measures among maps, we generalized land cover classifications
543 using dominant life form types (LFT). Although other generalizations are possible, LFTs
544 represent the most general and unambiguous common denominator of current global
545 maps. There have been growing international efforts to promote a common land cover
546 language (LCCS, Di Gregorio 2005) and to provide translations between existing legends
547 (Herold et al. 2006; Thomlinson et al. 1999). Using the LCCS system, Herold et al.
548 (2008) created a generalized legend for the IGBP, GLC-2000 and the UMD
549 classification. Their generalized legend maintains a relatively detailed land cover scheme
550 that includes 13 classes, but does not eliminate categorical ambiguities among the tree
551 life form types. Evidently, the comparability of existing global land cover maps is limited

552 as a result of the different classification systems and class definitions. Current maps use
553 different tree cover and tree height thresholds to distinguish between tree and non-tree
554 classes (10% and 2 m in MODIS IGBP, 20% and a 5-m in GLC-2000 for Northern
555 Eurasia (Bartalev et al. 2003), and 15% and 5 m in GLOBCOVER). Considering the vast
556 diversity of biomes and vegetation types on Earth, global land cover mapping efforts face
557 a difficult task. Classes representing mixtures of different land cover reflect difficulties of
558 map developers to spectrally distinguish between the underlying cover types.
559 Nevertheless, future mapping efforts should focus on standardized classification systems
560 to improve compatibility with other maps. MODIS Land Cover for Collection 6 plans to
561 use an LCCS-based classification (Friedl et al. 2010).

562 Our approach builds on earlier global map validation efforts that relied on Landsat-based
563 maps as reference data (Cohen et al. 2006; Cohen et al. 2003). The combination of higher
564 resolution reference maps and a standardized LCCS-based classification provides a
565 flexible validation framework for assessing coarse resolution maps of different spatial
566 resolutions and thematic detail. A disadvantage is the limited number of test sites and
567 their opportunistic selection precludes the conclusive assessment of coarse resolution
568 map performance across the entire region of Northern Eurasia. However, the results give
569 an indication of the differences, strengths and weaknesses of the examined maps at
570 specific locations, and the relative magnitude of different types of errors likely to be
571 found in the maps. Furthermore, the comparison of different accuracy metrics at selected
572 locations provides insights into interpretation of commonly reported global map
573 accuracies.

574 The need for standardized quantitative assessment of available land cover maps is widely
575 recognized and different aspects of this task have been studied in recent years (e.g.
576 Herold et al. 2008; Jung et al. 2006; See and Fritz 2006). Because the collection of
577 reference data requires a significant investment, it is desirable to develop standards that
578 are not limited to a particular map, but can be ‘re-used’ and extended to accommodate
579 different classifications and spatial resolutions (Justice et al. 2000). While sampling
580 designs for map validation are well understood (Strahler et al. 2006), methods for relating
581 maps of different spatial and thematic resolution have not been studied to the same extent
582 and community consensus on the strengths and weaknesses of different approaches is still
583 evolving. Thematic map products that focus on a single class represent a simpler case
584 (e.g. Roy and Boschetti 2009), but land cover maps are inherently more complex, which
585 makes evaluations and comparisons challenging.

586 Differences among land cover maps have important implications for biogeochemical (e.g.
587 Potter et al. 2008) and habitat models (e.g. Kuemmerle et al. in press) that use these
588 products. A simple analysis that extrapolated results of biogeochemical modeling for the
589 Arctic region of Northern Eurasia (North of 60 degrees) showed that a very different
590 picture of the regional carbon (C) balance emerges when different vegetation maps are
591 used as model inputs (Krankina et al. 2010): The estimate of C stock in live vegetation
592 based on the GLC-2000 map (24 Pg C) is 40% higher than the estimate based on the
593 MODIS plant functional type (PFT) map (17 Pg C). While the estimates of the total
594 change in live vegetation C stocks are very similar for both maps (0.2 Pg yr^{-1} C sink), the
595 attribution of the projected C sink is quite different depending on the map used: based on
596 GLC-2000 map most of the C accumulation occurs in tree-dominated ecosystems while

597 simulations using the MODIS PFT map attribute most of the C sink to shrub vegetation.
598 The significant role of land cover map selection on forest biomass estimates in Russian
599 forests was also reported by Houghton et al. (2007).

600 Globally consistent vegetation maps with known accuracy are a fundamental requirement
601 for global change research and sound policies to address global change. Growing
602 recognition of the role of terrestrial ecosystems and land use in the global carbon cycle
603 (IPCC 2007) places new demands on the accuracy of products derived from satellite
604 observations. Methods for independent map validation have been actively studied in
605 recent years but many issues remain unresolved, including design of map legends that
606 lend themselves to uniform aggregation (i.e., LCCS), consensus on metrics of agreement
607 between fine-resolution reference data and coarser global maps, and support for a
608 globally distributed set of test sites against which all maps can be compared (Justice et al.
609 2000).

610 5 Acknowledgements

611 The research was supported by the Land Cover/Land-Use Change Program of the
612 National Aeronautics and Space Administration (grant numbers NNG06GF54G and
613 NNX09AK88G) and in part by the Asia-Pacific Network for Global Change Research.
614 We like to thank Dr. Curtis Woodcock for his advice in the early planning of this study,
615 and Gretchen Bracher for preparing most of the graphs in this paper.

616 References:

- 617 Alexeyev, V.A., & Birdsey, R.A. (1998). Carbon storage in forests and peatlands of
618 Russia. In (p. 137). Radnor: U.S. Department of Agriculture, Forest Service, Northern
619 Research Station
- 620 Arino, O., Bicheron, P., Achard, F., Latham, J., Witt, R., & Weber, J.L. (2008).
621 GLOBCOVER The most detailed portrait of Earth. *Esa Bulletin-European Space Agency*,
622 24-31
- 623 Bartalev, S.A., Belward, A.S., Erchov, D.V., & Isaev, A.S. (2003). A new SPOT4-
624 VEGETATION derived land cover map of Northern Eurasia. *International Journal of*
625 *Remote Sensing*, 24, 1977-1982
- 626 Bartholome, E., & Belward, A.S. (2005). GLC2000: a new approach to global land cover
627 mapping from Earth observation data. *International Journal of Remote Sensing*, 26,
628 1959-1977
- 629 Bicheron, P., Defourny, P., Brockmann, C., Schouten, L., Vancutsem, C., Huc, M.,
630 Bontemps, S., Leroy, M., Achard, F., Herold, M., Ranera, F., & Arino, O. (2008).
631 GLOBCOVER: Products Description and Validation Report. In (p. 47). Toulouse,
632 France: POSTEL
- 633 Boschetti, L., Flasse, S.P., & Brivio, P.A. (2004). Analysis of the conflict between
634 omission and commission in low spatial resolution dichotomic thematic products: The
635 Pareto Boundary. *Remote Sensing of Environment*, 91, 280-292
- 636 Chapin, F.S., Sturm, M., Serreze, M.C., McFadden, J.P., Key, J.R., Lloyd, A.H.,
637 McGuire, A.D., Rupp, T.S., Lynch, A.H., Schimel, J.P., Beringer, J., Chapman, W.L.,
638 Epstein, H.E., Euskirchen, E.S., Hinzman, L.D., Jia, G., Ping, C.L., Tape, K.D.,
639 Thompson, C.D.C., Walker, D.A., & Welker, J.M. (2005). Role of land-surface changes
640 in Arctic summer warming. *Science*, 310, 657-660
- 641 Cohen, J. (1960). A coefficient of agreement for nominal scales. *Educational and*
642 *Psychological Measurement*, 20, 37-46
- 643 Cohen, W.B., Maieresperger, T.K., Turner, D.P., Ritts, W.D., Pflugmacher, D., Kennedy,
644 R.E., Kirschbaum, A., Running, S.W., Costa, M., & Gower, S.T. (2006). MODIS land
645 cover and LAI collection 4 product quality across nine sites in the western hemisphere.
646 *IEEE Transactions on Geoscience and Remote Sensing*, 44, 1843-1857
- 647 Cohen, W.B., Maieresperger, T.K., Yang, Z.Q., Gower, S.T., Turner, D.P., Ritts, W.D.,
648 Berterretche, M., & Running, S.W. (2003). Comparisons of land cover and LAI estimates
649 derived from ETM plus and MODIS for four sites in North America: a quality assessment
650 of 2000/2001 provisional MODIS products. *Remote Sensing of Environment*, 88, 233-255

- 651 Czaplewski, R. (1994). Variance Approximations for Assessments of Classification
652 Accuracy. In (p. 29). Fort Collins: US Department of Agriculture, Forest Service
- 653 DeFries, R.S., & Townshend, J.R.G. (1994). NDVI derived land cover classifications at a
654 global scale. *International Journal of Remote Sensing*, 15, 3567-3586
- 655 Di Gregorio, A. (2005). Land cover classification system: Classification concepts and
656 user manual for software -- version 2. In (p. 190). Rome, Italy: Food & Agriculture
657 Organization of the United Nations
- 658 Foody, G.M. (2002). Status of land cover classification accuracy assessment. *Remote
659 Sensing of Environment*, 80, 185-201
- 660 Forbes, B.C., Fresco, N., Shvidenko, A., Danell, K., & Chapin, F.S. (2004). Geographic
661 variations in anthropogenic drivers that influence the vulnerability and resilience of
662 social-ecological systems. *Ambio*, 33, 377-382
- 663 Frey, K.E., & Smith, L.C. (2007). How well do we know northern land cover?
664 Comparison of four global vegetation and wetland products with a new ground-truth
665 database for West Siberia. *Global Biogeochemical Cycles*, 21, -
- 666 Friedl, M.A., McIver, D.K., Hodges, J.C.F., Zhang, X.Y., Muchoney, D., Strahler, A.H.,
667 Woodcock, C.E., Gopal, S., Schneider, A., Cooper, A., Baccini, A., Gao, F., & Schaaf,
668 C.B. (2002). Global land cover mapping from MODIS: algorithms and early results.
669 *Remote Sensing of Environment*, 83, 287-302
- 670 Friedl, M.A., Sulla-Menashe, D., Tan, B., Schneider, A., Ramankutty, N., Sibley, A., &
671 Huang, X.M. (2010). MODIS Collection 5 global land cover: Algorithm refinements and
672 characterization of new datasets. *Remote Sensing of Environment*, 114, 168-182
- 673 Fritz, S., & See, L. (2008). Identifying and quantifying uncertainty and spatial
674 disagreement in the comparison of Global Land Cover for different applications. *Global
675 Change Biology*, 14, 1057-1075
- 676 Giri, C., Zhu, Z.L., & Reed, B. (2005). A comparative analysis of the Global Land Cover
677 2000 and MODIS land cover data sets. *Remote Sensing of Environment*, 94, 123-132
- 678 Groisman, P.Y., Clark, E.A., Kattsov, V.M., Lettenmaier, D.P., Sokolik, I.N., Aizen,
679 V.B., Cartus, O., Chen, J.Q., Conard, S., Katzenberger, J., Krankina, O., Kukkonen, J.,
680 Machida, T., Maksyutov, S., Ojima, D., Qi, J.G., Romanovsky, V.E., Santoro, M.,
681 Schmullius, C.C., Shiklomanov, A.I., Shimoyama, K., Shugart, H.H., Shuman, J.K.,
682 Sofiev, M.A., Sukhinin, A.I., Vorosmarty, C., Walker, D., & Wood, E.F. (2009). The
683 Northern Eurasia Earth Science Partnership an Example of Science Applied to Societal
684 Needs. *Bulletin of the American Meteorological Society*, 90, 671-+
- 685 Hansen, M.C., DeFries, R.S., Townshend, J.R.G., & Sohlberg, R. (2000). Global land
686 cover classification at 1 km spatial resolution using a classification tree approach.
687 *International Journal of Remote Sensing*, 21, 1331-1364

- 688 Hansen, M.C., DeFries, R.S., Townshend, J.R.G., Sohlberg, R., Dimiceli, C., & Carroll,
689 M.L. (2002). Towards an operational MODIS continuous field of percent tree cover
690 algorithm: examples using AVHRR and MODIS data. *Remote Sensing of Environment*,
691 83, 303-319
- 692 Hansen, M.C., Townshend, J.R.G., Defries, R.S., & Carroll, M. (2005). Estimation of tree
693 cover using MODIS data at global, continental and regional/local scales. *International
694 Journal of Remote Sensing*, 26, 4359-4380
- 695 Heikkinen, J.E.P., Virtanen, T., Huttunen, J.T., Elsakov, V., & Martikainen, P.J. (2004).
696 Carbon balance in East European tundra. *Global Biogeochemical Cycles*, 18, -
- 697 Herold, M., Mayaux, P., Woodcock, C.E., Baccini, A., & Schmullius, C. (2008). Some
698 challenges in global land cover mapping: An assessment of agreement and accuracy in
699 existing 1 km datasets. *Remote Sensing of Environment*, 112, 2538-2556
- 700 Herold, M., Woodcock, C., diGregorio, A., Mayaux, P., Belward, A.S., Latham, J., &
701 Schmullius, C.C. (2006). A Joint Initiative for Harmonization and Validation of Land
702 Cover Datasets. *Ieee Transactions on Geoscience and Remote Sensing*, 44, 1719-1727
- 703 Houghton, R.A., Butman, D., Bunn, A., Krankina, O., Schlesinger, P., & Stone, T.A.
704 (2007). Mapping Russian Forest Biomass with Data from Satellites and Forest
705 Inventories. *Environmental Research Letters*, 2, 7pp.
- 706 Justice, C.O., Belward A., Morisette J., Lewis P., Privette J., Baret F. (2000).
707 Developments in the validation of satellite products for the study of the land surface.
708 *International Journal of Remote Sensing*, 21(17), 3383-3390.
- 709 Jung, M., Henkel, K., Herold, M., & Churkina, G. (2006). Exploiting synergies of global
710 land cover products for carbon cycle modeling. *Remote Sensing of Environment*, 101,
711 534-553
- 712 Kharuk, V.I., Ranson, K.J., Kozuhovskaya, A.G., Kondakov, Y.P., & Pestunov, I.A.
713 (2004). NOAA/AVHRR satellite detection of Siberian silkmouth outbreaks in eastern
714 Siberia. *International Journal of Remote Sensing*, 25, 5543-5555
- 715 Kharuk, V.I., Ranson, K.J., Kuz'michev, V.V., & Im, S. (2003). Landsat-based analysis
716 of insect outbreaks in southern Siberia. *Canadian Journal of Remote Sensing*, 29, 286-
717 297
- 718 Krankina, O., Pflugmacher, D., Hayes, D.J., McGuire, A.D., Hansen, M., Haeme, T.,
719 Elsakov, V., & Nelson, P. (2010). Vegetation Cover in the Eurasian Arctic: Distribution,
720 Monitoring, and Role in Carbon Cycling. In G. Gutman & A. Reissell (Eds.), *Arctic land
721 cover and land use in a changing climate*
- 722 Krankina, O.N., Bergen, K.M., Sun, G., Masek, J.G., Shugart, H.H., Kharuk, V.,
723 Kasischke, E., Cohen, W.B., Oetter, D.R., & Duane, M.V. (2004a). Northern Eurasia:
724 Remote sensing of boreal forests in selected regions. In G. Gutman, A.C. Janetos, C.O.

- 725 Justice, E.F. Moran, J.F. Mustard, R.R. Rindfuss, D. Skole, B.L. Turner II & M.A.
726 Cochrane (Eds.), *Land Change Science: Observing, Monitoring and Understanding*
727 *Trajectories of Change on the Earth's Surface* (pp. 123-138). Berlin: Springer
- 728 Krankina, O.N., Harmon, M.E., Cohen, W.B., Oetter, D.R., Zyrina, O., & Duane, M.V.
729 (2004b). Carbon stores, sinks, and sources in forests of northwestern Russia: Can we
730 reconcile forest inventories with remote sensing results? *Climatic Change*, 67, 257-272
- 731 Krankina, O.N., Pflugmacher, D., Friedl, M., Cohen, W.B., Nelson, P., & Baccini, A.
732 (2008). Meeting the challenge of mapping peatlands with remotely sensed data.
733 *Biogeosciences*, 5, 1809-1820
- 734 Kuemmerle, T., Hostert, P., Radeloff, V.C., Perzanowski, K., & Kruhlov, I. (2007). Post-
735 socialist forest disturbance in the Carpathian border region of Poland, Slovakia, and
736 Ukraine. *Ecological Applications*, 17, 1279-1295
- 737 Kuemmerle, T., Hostert, P., Radeloff, V.C., van der Linden, S., Perzanowski, K., &
738 Kruhlov, I. (2008). Cross-border comparison of post-socialist farmland abandonment in
739 the Carpathians. *Ecosystems*, 11, 614-628
- 740 Kuemmerle, T., Chaskovskyy, O., Knorn, J., Radeloff, V.C., Kruhlov, I., Keeton, W.S.,
741 & Hostert, P. (2009). Forest cover change and illegal logging in the Ukrainian
742 Carpathians in the transition period from 1988 to 2007. *Remote Sensing of Environment*,
743 113, 1194-1207
- 744 Kuemmerle, T., Radeloff, V.C., Perzanowski, K., Kozlo, P., Sipko, T., Khoyetskyy, P.,
745 Bashta, A.-T., Chikurova, E., Parnikoza, I., Baskin, L., Angelstam, P., & Waller, D.M.
746 (in press). Predicting potential European bison habitat across its former range. *Ecological*
747 *Applications*
- 748 Latifovic, R., & Olthof, I. (2004). Accuracy assessment using sub-pixel fractional error
749 matrices of global land cover products derived from satellite data. *Remote Sensing of*
750 *Environment*, 90, 153-165
- 751 Loveland, T.R., Reed, B.C., Brown, J.F., Ohlen, D.O., Zhu, Z., Yang, L., & Merchant,
752 J.W. (2000). Development of a global land cover characteristics database and IGBP
753 DISCover from 1 km AVHRR data. *International Journal of Remote Sensing*, 21, 1303-
754 1330
- 755 Mayaux, P., Eva, H., Gallego, J., Strahler, A.H., Herold, M., Agrawal, S., Naumov, S.,
756 DeMiranda, E.E., DiBella, C.M., Ordoyne, C., Kopin, I., & Roy, P.S. (2006). Validation
757 of the Global Land Cover 2000 Map. *Ieee Transactions on Geoscience and Remote*
758 *Sensing*, 44, 1728-1739
- 759 Pflugmacher, D., Krankina, O.N., & Cohen, W.B. (2007). Satellite-based peatland
760 mapping: Potential of the MODIS sensor. *Global and Planetary Change*, 56, 248-257

761 Potter, C., Gross, P., Klooster, S., Fladeland, M., & Genovese, V. (2008). Storage of
762 carbon in US forests predicted from satellite data, ecosystem modeling, and inventory
763 summaries. *Climatic Change*, 90, 269-282

764 Roy, D.P., & Boschetti, L. (2009). Southern Africa Validation of the MODIS, L3JRC,
765 and GlobCarbon Burned-Area Products. *Ieee Transactions on Geoscience and Remote*
766 *Sensing*, 47, 1032-1044

767 See, L.M., & Fritz, S. (2006). A Method to Compare and Improve Land Cover Datasets:
768 Application to the GLC-2000 and MODIS Land Cover Products. *Ieee Transactions on*
769 *Geoscience and Remote Sensing*, 44, 1740-1746

770 Stehman, S.V., & Czaplewski, R.L. (1998). Design and analysis for thematic map
771 accuracy assessment: Fundamental principles. *Remote Sensing of Environment*, 64, 331-
772 344

773 Strahler, A., Boschetti, L., Foody, G.M., Friedl, M.A., Hansen, M.C., Herold, M.,
774 Mayaux, P., Morisette, J.T., Stehman, S.V., & Woodcock, C. (2006). Global land cover
775 validation: Recommendations for evaluation and accuracy assessment of global land
776 cover maps. In (p. 58): European Communities

777 Thomlinson, J.R., Bolstad, P.V., & Cohen, W.B. (1999). Coordinating methodologies for
778 scaling landcover classifications from site-specific to global: Steps toward validating
779 global map products. *Remote Sensing of Environment*, 70, 16-28

780 Townshend, J.R.G., Huang, C., Kalluri, S.N.V., Defries, R.S., Liang, S., & Yang, K.
781 (2000). Beware of per-pixel characterization of land cover. *International Journal of*
782 *Remote Sensing*, 21, 839-843

783 Turner, D.P., Cohen, W.B., & Kennedy, R.E. (2000). Alternative spatial resolutions and
784 estimation of carbon flux over a managed forest landscape in Western Oregon.
785 *Landscape Ecology*, 15, 441-452

786

787

788

Table 1. Aligning the legends of global maps: dominant life form type (LFT) and corresponding land cover classes from GLC-2000, GLOBCOVER & MODIS IGBP

Dominant LFT	GLC-2000	GLOBCOVER	MODIS IGBP
Tree	[1] Tree Cover; broadleaved; evergreen	[40] Broadleaved evergreen or semi-deciduous forest, closed to open	[1] Evergreen Needleleaf Forest
	[2] Tree Cover; broadleaved; deciduous; closed	[50] Broadleaved deciduous forest, closed	[2] Evergreen Broadleaf Forest
	[3] Tree Cover; broadleaved; deciduous; open	[60] Broadleaved deciduous forest/woodland, open	[3] Deciduous Needleleaf Forest
	[4] Tree Cover; needle-leaved; evergreen	[70] Needleleaved evergreen forest, closed	[4] Deciduous Broadleaf Forest
	[5] Tree Cover; needle-leaved; deciduous	[90] Needleleaved deciduous or evergreen forest, open	[5] Mixed Forest
	[6] Tree Cover; mixed leaf type	[100] Mixed broadleaved & needleleaved forest, closed-open	[8] Woody Savannas
	[7] Tree Cover; regularly flooded; fresh water	[160] Broadleaved forest regularly flooded, closed to open	[9] Savannas
	[8] Tree Cover; regularly flooded; saline water		
	[9] Mosaic: Tree cover; Other natural vegetation		
	[10] Tree Cover; burnt		
Shrub	[11] Shrub Cover; closed-open; evergreen	[130] Shrubland, closed to open	[6] Closed Shrublands
	[12] Shrub Cover; closed-open; deciduous		[7] Open Shrublands
Herbaceous	[13] Herbaceous Cover; closed-open	[11] Post-flooding or irrigated croplands (or aquatic)	[10] Grasslands
	[16] Cultivated and managed areas	[140] Herbaceous vegetation, closed to open	[12] Croplands
		[14] Rainfed croplands	
Barren	[14] Sparse herbaceous or sparse shrub cover vegetation cover between 1% and 10-20% vegetation cover	[150] Sparse vegetation (<15%)	[16] Barren or Sparsely Vegetated
	[22] Artificial surfaces and associated areas	[190] Artificial surfaces and associated areas	[13] Urban and Built-Up
	[19] Bare Areas	[200] Bare areas	
	[21] Snow and Ice	[220] Permanent snow and ice	[15] Snow and Ice
Mosaic	[15] Regularly flooded shrub and-or herbaceous cover	[20] Mosaic cropland (50-70%) / vegetation (grassland/ shrubland/ forest) (20-50%)	[11] Permanent Wetlands
	[17] Mosaic: Cropland; Tree Cover; Other natural vegetation	[30] Mosaic vegetation (grassland/ shrubland/ forest) (50-70%) / cropland (20-50%)	[14] Cropland-Natural Vegetation Mosaic
	[18] Mosaic: Cropland; Shrub and-or Herbaceous cover	[110] Mosaic forest or shrubland (50-70%) / grassland (20-50%)	
		[120] Mosaic grassland (50-70%) / forest or shrubland (20-50%)	
		[170] Broadleaved forest or shrubland permanently flooded, closed	
	[180] Grassland or woody vegetation on regularly flooded or waterlogged soil, closed-open		
Water	[20] Water Bodies	[210] Water bodies	[0] Water Bodies

Table 2. Test site information

Site	Location	Latitude, Longitude	Landsat Path/Row	Landsat Image Date	Mean Temperature (°C)			Mean Annual Precipitation (mm)	Elevation asl (m)
					January	July	Annual		
CARP	Carpathians (border region of Poland, Slovakia, Ukraine)	48.87, 22.40	186/20	6-Jun-2000 21-Aug-2000 30- Sep-2000	-7	19	6	900-1200	100-2000
STPB	St. Petersburg Region (Russia)	60.09, 31.27	184/18	2-Jun-2002	-10	17	4	600-800	0-250
KOMI	Komi Republic (Russia)	66.94, 57.10	171/13	1-Jun-2000 19- Jul-2000	-19	12	-5	360-500	20-240
VASY	Vasyugan Basin, Tomsk Region, West Siberia (Russia)	57.32, 82.09	150/20	16-Sep-1999	-18	18	0	450-550	110-130
PRIA	Priangarie, Krasnoyarsk Region, East Siberia (Russia)	57.30, 95.91	141/20	18-Aug-2000	-22	18	3	400-450	100-600
CHIT	Chita Region and Buriat Republic, East Siberia (Russia)	51.69, 111.64	129/24	11-Jun-2000	-26	15	-4	380	600-1500

Table 3. Error matrix of dominant life form types for Landsat-based reference maps at test sites.

Predicted		Observed Class					
Class	Site	Tree	Shrub	Herb	Barren	Water	
Tree	STPB	2176		18			
	CARP	466	7	7		4	
	KOMI	289	22			1	
	PRIA	851	7	7			
	CHIT	210	3	3		2	
	VASY	179	3	2			
Shrub	STPB		44	6	1		
	CARP	2	59	19	2	2	
	KOMI	8	39	8	1		
	PRIA	2	25	13	1		
	CHIT	18	26	1			
	VASY	7	45	3			
Herbaceous	STPB	6	5	58	1		
	CARP	1	26	346	1		
	KOMI	12	1	14	15	3	
	PRIA	8	1	658			
	CHIT	2	7	37	8		
	VASY	1	10	52	1		
Barren	STPB		1	5	380		
	CARP		3	3	29	1	
	KOMI			15	41	1	
	PRIA		7	13	199		
	CHIT			3	22		
	VASY				32		
Water	STPB					116	
	CARP					22	
	KOMI	2				34	
	PRIA					274	
	CHIT					32	
	VASY					24	
Percent Correct	STPB	1.00	0.88	0.67	0.99	1.00	0.98
	CARP	0.99	0.62	0.92	0.91	0.76	0.92
	KOMI	0.93	0.63	0.38	0.72	0.87	0.8
	PRIA	0.99	0.63	0.95	1.00	1.00	0.97
	CHIT	0.91	0.72	0.84	0.73	0.94	0.87
	VASY	0.96	0.78	0.91	0.97	1.00	0.92
	All Sites	0.98	0.70	0.90	0.96	0.97	0.91

Table 4. Overall agreement between reference maps and coarse resolution land cover products and Kappa statistic for per-pixel comparisons of dominant life form types at test sites

Site	GLC2000		GLOBCOVER		MODIS V4		MODIS V5	
	Agree- ment	Kappa	Agree- ment	Kappa	Agree- ment	Kappa	Agree- ment	Kappa
All pixels								
Carpathians	0.69	0.45	0.73	0.57	0.75	0.56	0.87	0.79
Chita	0.76	0.40	0.83	0.51	0.72	0.37	0.67	0.35
Komi	0.58	0.41	0.34	0.22	0.42	0.16	0.49	0.28
Priangarie	0.84	0.39	0.85	0.49	0.80	0.35	0.86	0.51
St. Petersburg	0.74	0.51	0.69	0.48	0.67	0.36	0.75	0.54
Vasyugan	0.74	0.34	0.72	0.39	0.68	0.17	0.77	0.45
Total across sites	0.73	0.47	0.70	0.46	0.67	0.41	0.74	0.52
Pure pixels only								
Carpathians	0.95	0.87	0.89	0.78	0.98	0.94	0.99	0.97
Chita	0.94	0.69	0.94	0.71	0.92	0.65	0.85	0.52
Komi	0.91	0.77	0.66	0.48	0.86	0.70	0.84	0.68
Priangarie	0.98	0.68	0.94	0.62	0.97	0.54	0.98	0.82
St. Petersburg	0.97	0.91	0.91	0.78	0.96	0.88	0.96	0.89
Vasyugan	0.98	0.49	0.94	0.54	0.97	0.27	0.97	0.62
Total across sites	0.96	0.80	0.91	0.72	0.96	0.78	0.94	0.79

Table 5. Sub-pixel fractional error matrices based on dominant life form types of GLC-2000, GLOBCOVER, MODIS V4 and MODIS V5 (aggregated results with reference data from all test sites)

		Landsat land cover (km ²)						
		Trees	Shrubs	Herbaceous	Barren	Mosaics	Water	Commission
GLC-2000								
	Trees	88,307	11,900	16,103	844	0	987	0.24
	Shrubs	851	4,180	3,618	200	0	445	0.40
	Herbaceous	3,570	3,277	12,131	1,054	0	223	0.30
	Barren	160	162	867	378	0	60	0.77
	Mosaic	4,867	3,507	6,589	389	0	468	-
	Water	313	64	132	89	0	1,226	0.33
	Omission	0.05	0.67	0.53	0.87	0.00	0.64	
GLOBCOVER								
	Trees	83,479	10,010	11,752	589	0	796	0.20
	Shrubs	1	0	6	0	0	0	0.00
	Herbaceous	608	832	4,831	447	0	17	0.11
	Barren	3,817	8,236	11,999	1,198	0	754	0.95
	Mosaic	11,311	4,230	11,248	690	0	164	-
	Water	125	46	94	72	0	1,895	0.15
	Omission	0.05	0.82	0.60	0.60	0.00	0.48	
MODIS V4								
	Trees	83,933	9,524	12,947	827	0	710	0.22
	Shrubs	7,859	9,275	10,657	564	0	1,210	0.67
	Herbaceous	4,044	3,409	13,733	1,038	0	180	0.36
	Barren	133	152	254	340	0	54	0.64
	Mosaic	1,411	550	1,557	74	0	51	-
	Water	280	115	194	105	0	1,182	0.37
	Omission	0.13	0.57	0.61	0.88	0.00	0.65	
MODIS V5								
	Trees	84,465	9,207	11,100	775	0	1,209	0.20
	Shrubs	2,943	6,737	7,354	428	0	747	0.52
	Herbaceous	4,654	2,963	12,020	744	0	119	0.29
	Barren	154	295	537	592	0	38	0.63
	Mosaic	6,553	4,043	8,737	418	0	304	-
	Water	20	8	14	26	0	1,145	0.06
	Omission	0.08	0.54	0.48	0.80	0.00	0.68	

List of Figures:

Figure 1. Locations of reference sites: 1 - Carpathians, 2 - St. Petersburg, 3 - Komi, 4 - Vasyugan, 5 - Priangarie, 6 – Chita.

Figure 2. Examples of sub-fractional error matrices for sampling units equal to a) the global map resolution and b) blocks of 2 x 2 coarse resolution pixels. For pixel-blocks, row and column totals must be computed from the map statistics.

Figure 3. Relative frequency of dominant life form types in Northern Eurasia based on global land cover maps.

Figure 4. Distribution of dominant life form types for Northern Eurasia based on GLC-2000, GLOBCOVER, MODIS V4 and MODIS V5

Figure 5. Distribution of dominant life form types at reference sites

Figure 6. Predicted (global map) versus reference land cover area in percent of total test site area for GLC-2000, GLOBCOVER, MODIS V4, and MODIS V5 (water not shown for clarity; (a) all pixels, (b) pure pixels only)

Figure 7. Total agreement versus number of pure coarse resolution pixels at each site. Pure pixels are defined to contain at least 95% of a single land cover class in the reference data.

Figure 8. Relationship between total agreement and size of sample unit (blocks of 1x1 to 10x10 pixels)

Figure 9. Relationship between kappa agreement and size of sample unit (blocks of 1x1 to 10x10 pixels)

Figure 1 BW (PRINT)



a)

Reference pixels within sampling unit X

A	A	A	B
B	A	A	B
B	B	B	B
B	B	B	C

Global map pixels = sampling unit X'

A'	B'
B'	B'

Confusion matrix Y with $i=3$ rows and $j=3$ columns

	A	B	C	Σ
A'	3	1	0	4
B'	2	9	1	12
C'	0	0	0	0
Σ	5	8	1	

b)

Reference pixels within sampling unit X

A	A	A	B
B	A	A	B
B	B	B	B
B	B	B	C

Resampled global map pixels within sampling unit X'

A'	A'	B'	B'
A'	A'	B'	B'
B'	B'	B'	B'
B'	B'	B'	B'

Confusion matrix Y with $i=3$ rows and $j=3$ columns

	A	B	C	Σ
A'	4	$Y_{1,2}$	$Y_{1,3}$	4
B'	$Y_{2,1}$	10	$Y_{2,3}$	12
C'	$Y_{3,1}$	$Y_{3,2}$	0	0
Σ	5	8	1	

Figure 3 BW (PRINT)
[Click here to download high resolution image](#)

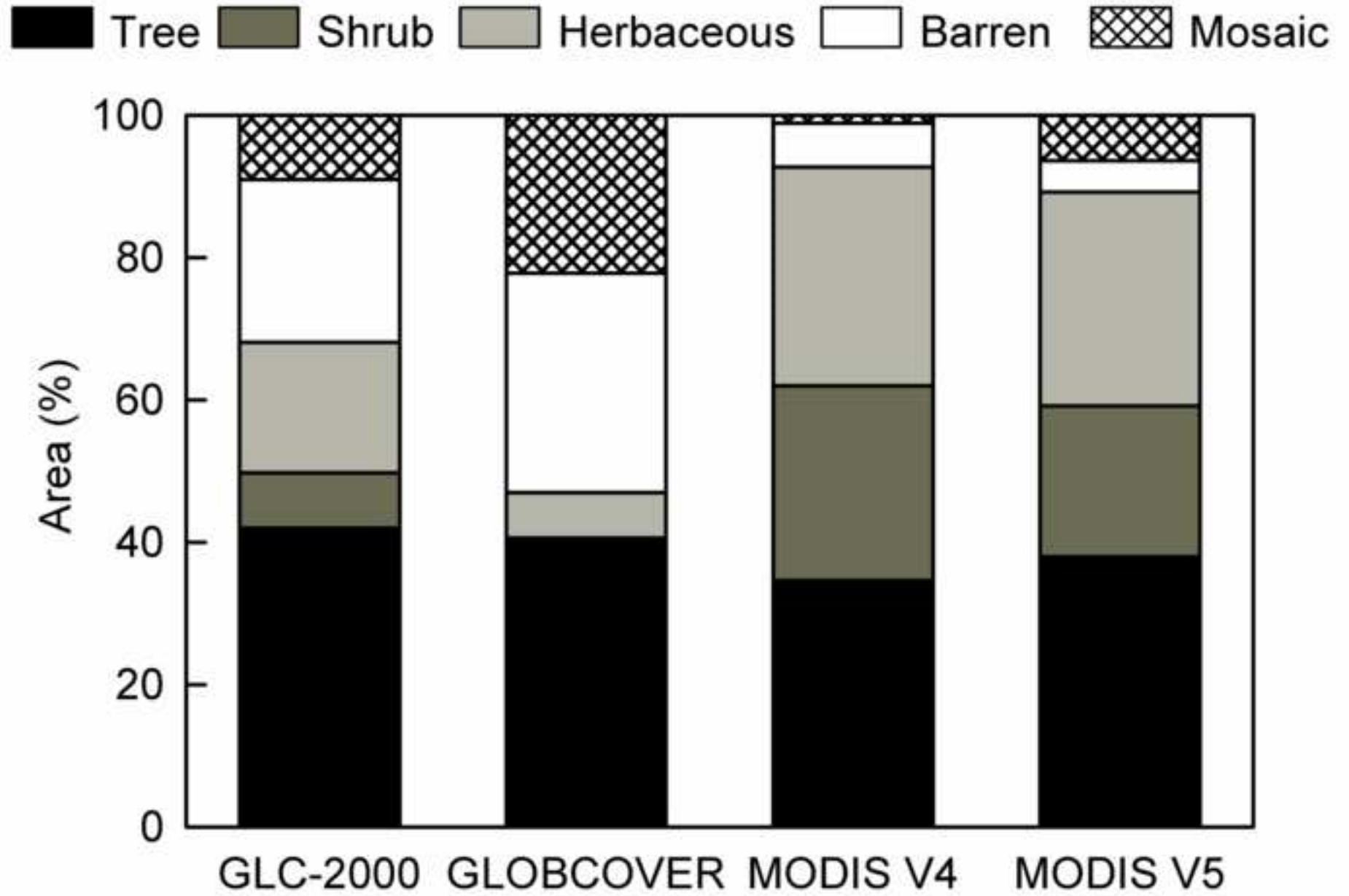


Figure 3 Color (ONLINE)
[Click here to download high resolution image](#)

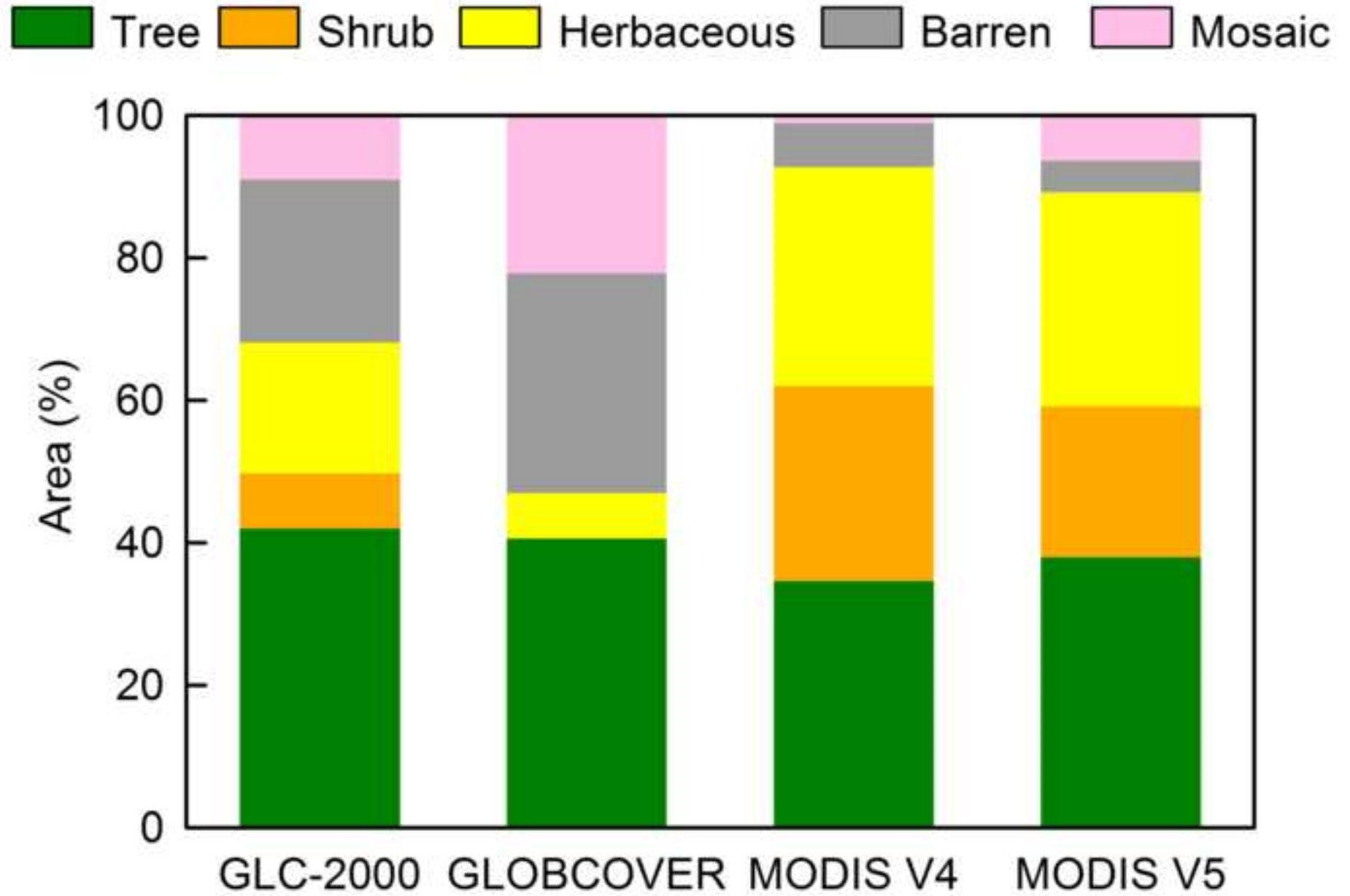


Figure 4 Color (PRINT)
[Click here to download high resolution image](#)

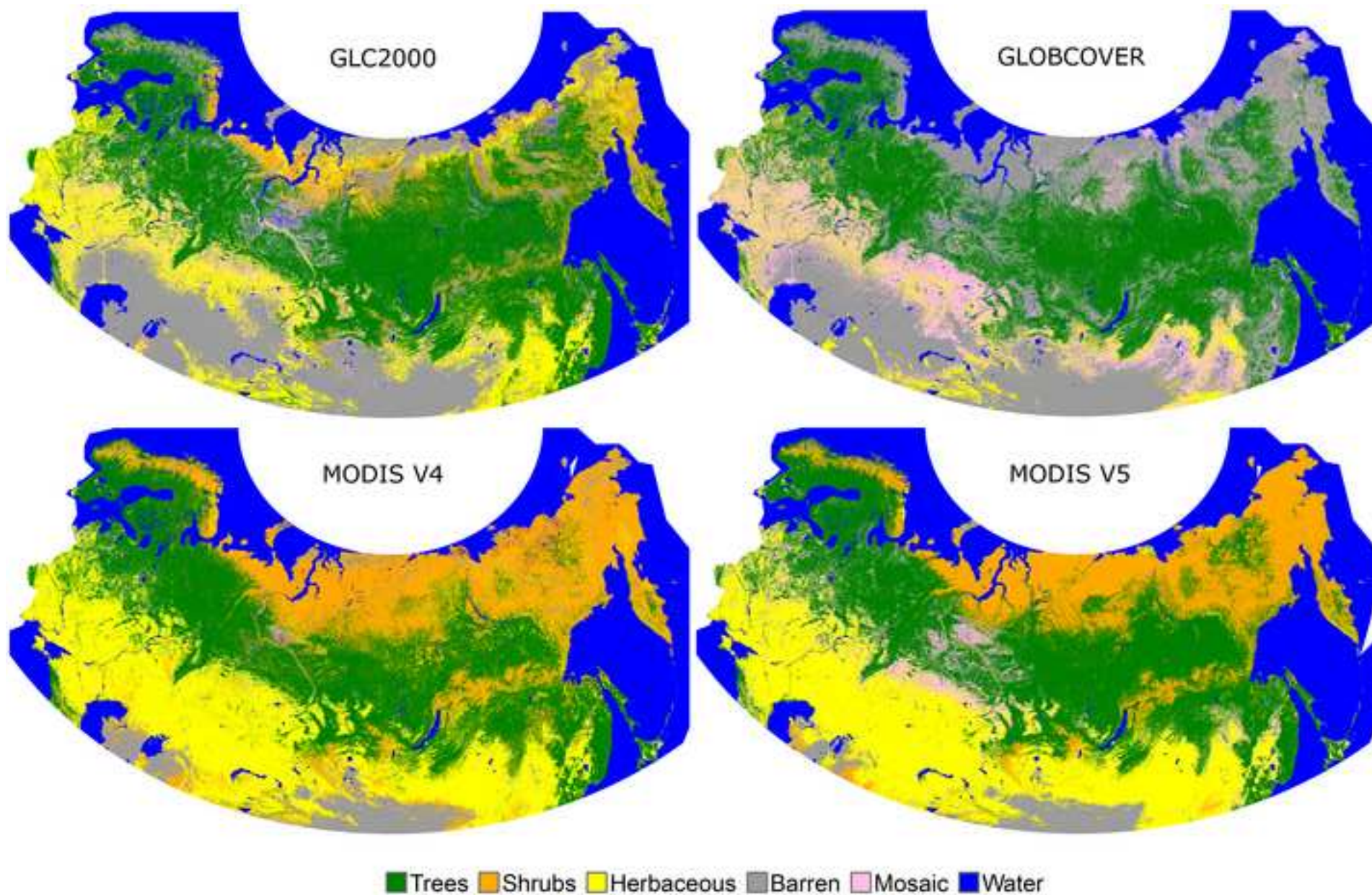


Figure 5 Color (PRINT)

[Click here to download high resolution image](#)

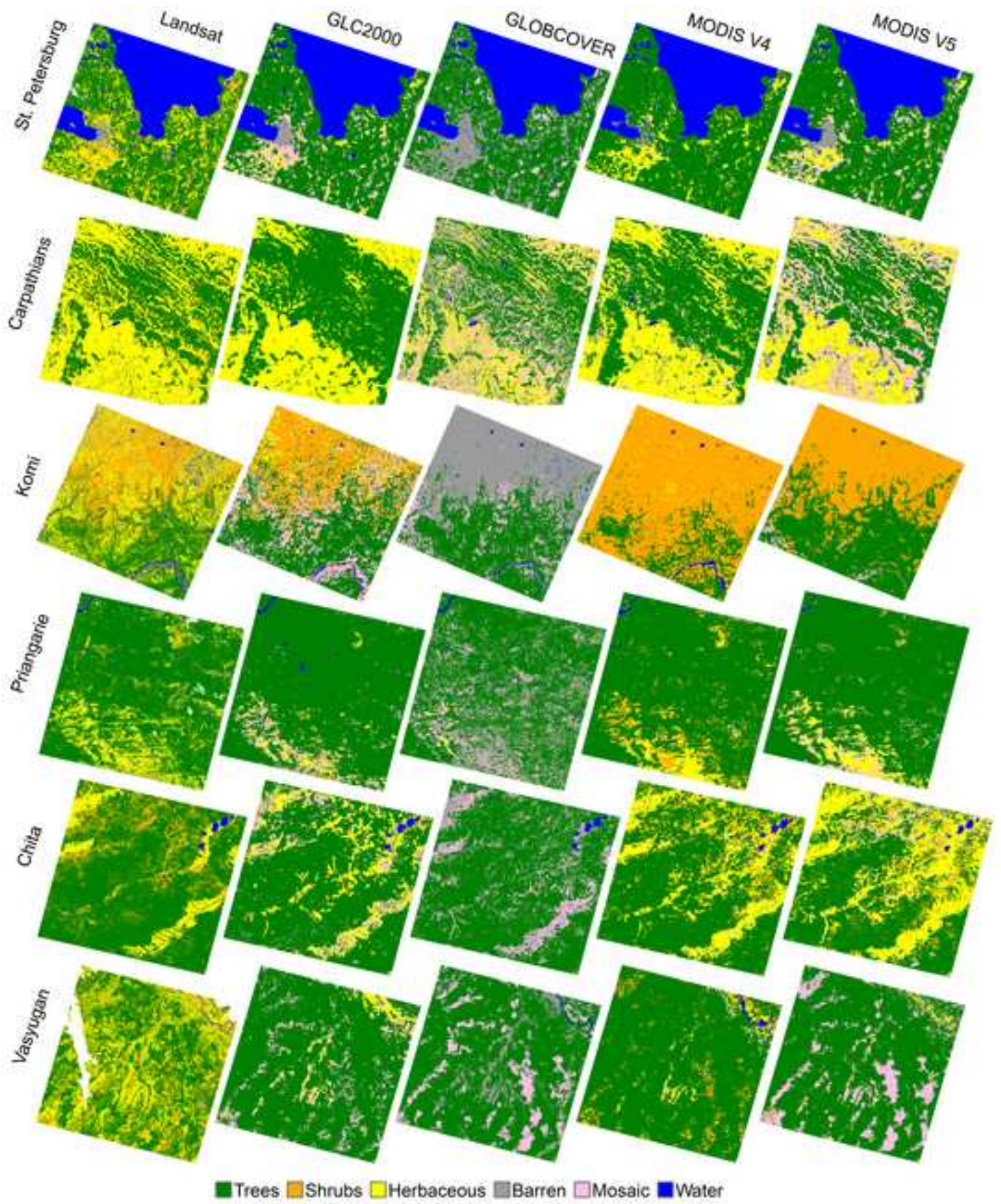


Figure 6 BW (PRINT)

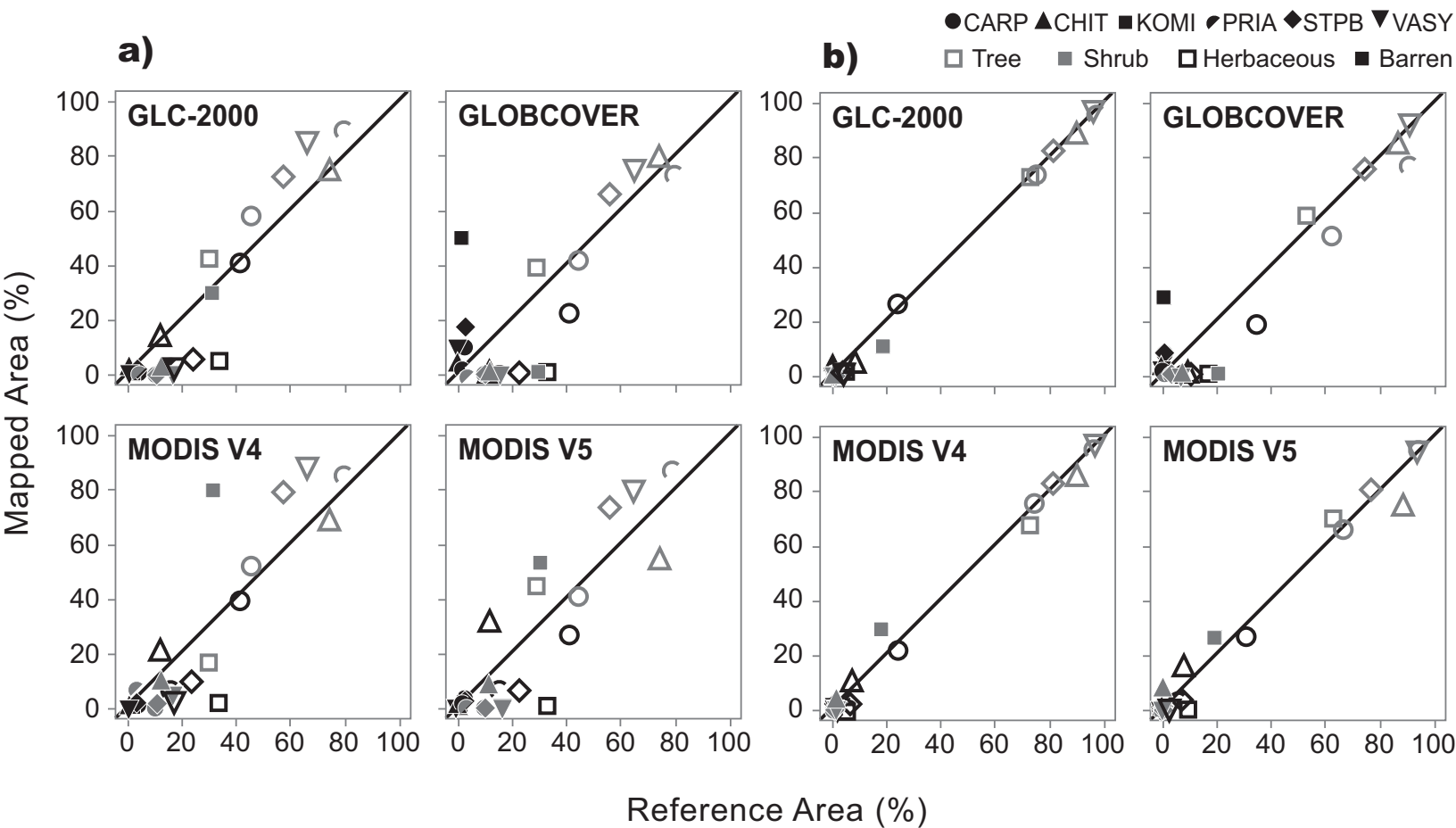


Figure 6 Color (ONLINE)

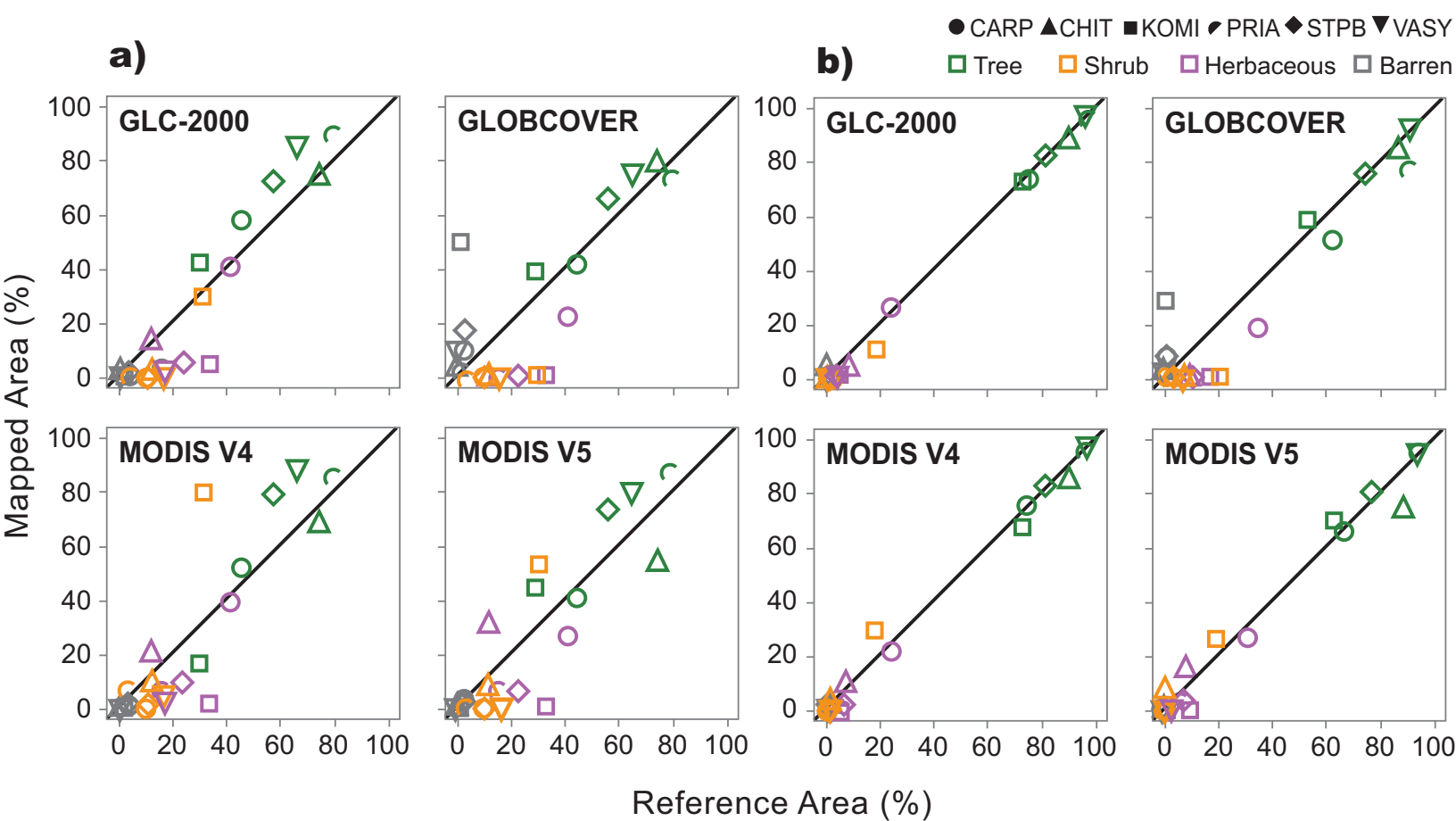


Figure 7 BW (PRINT)

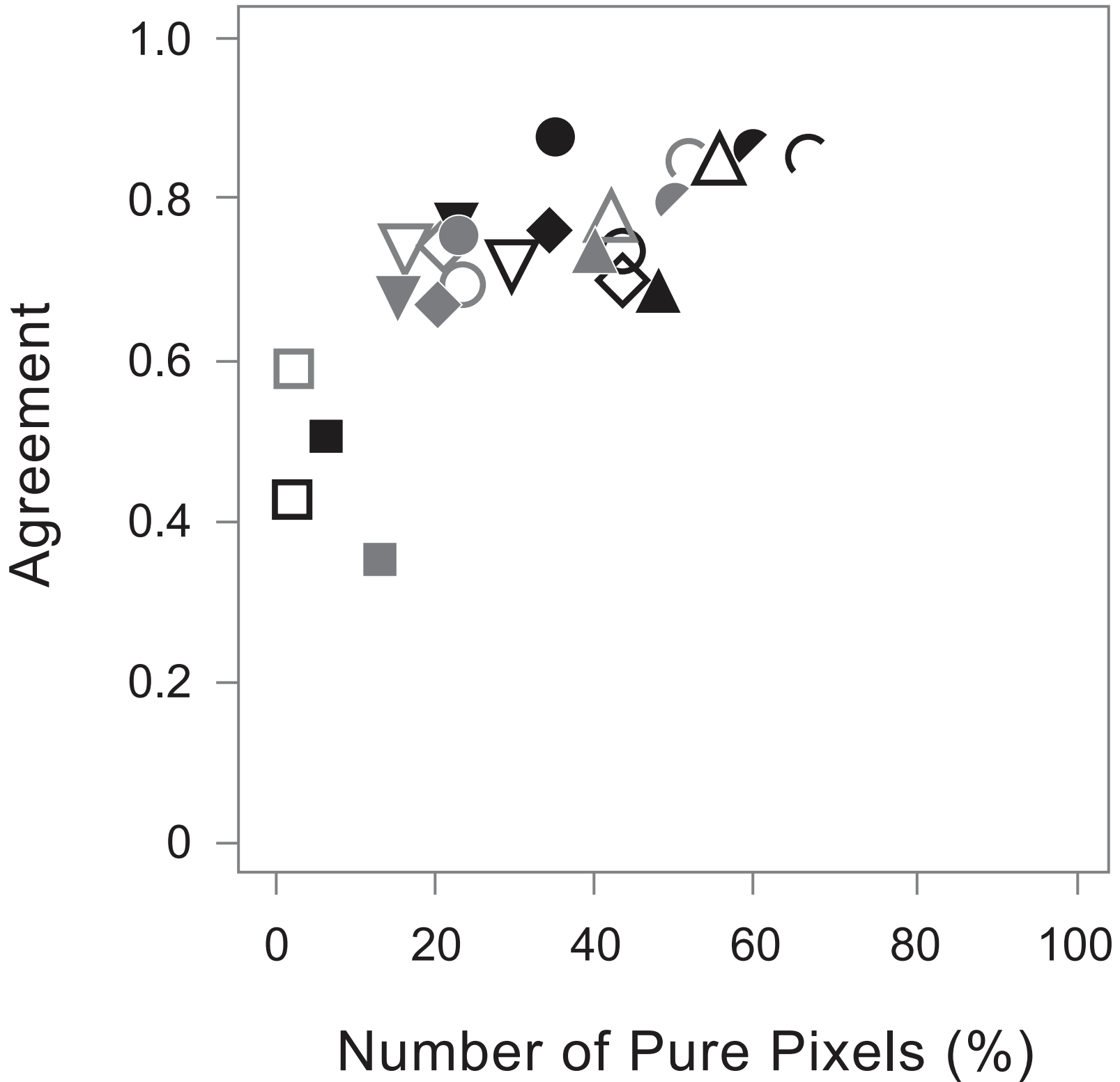


Figure 7 Color (ONLINE)

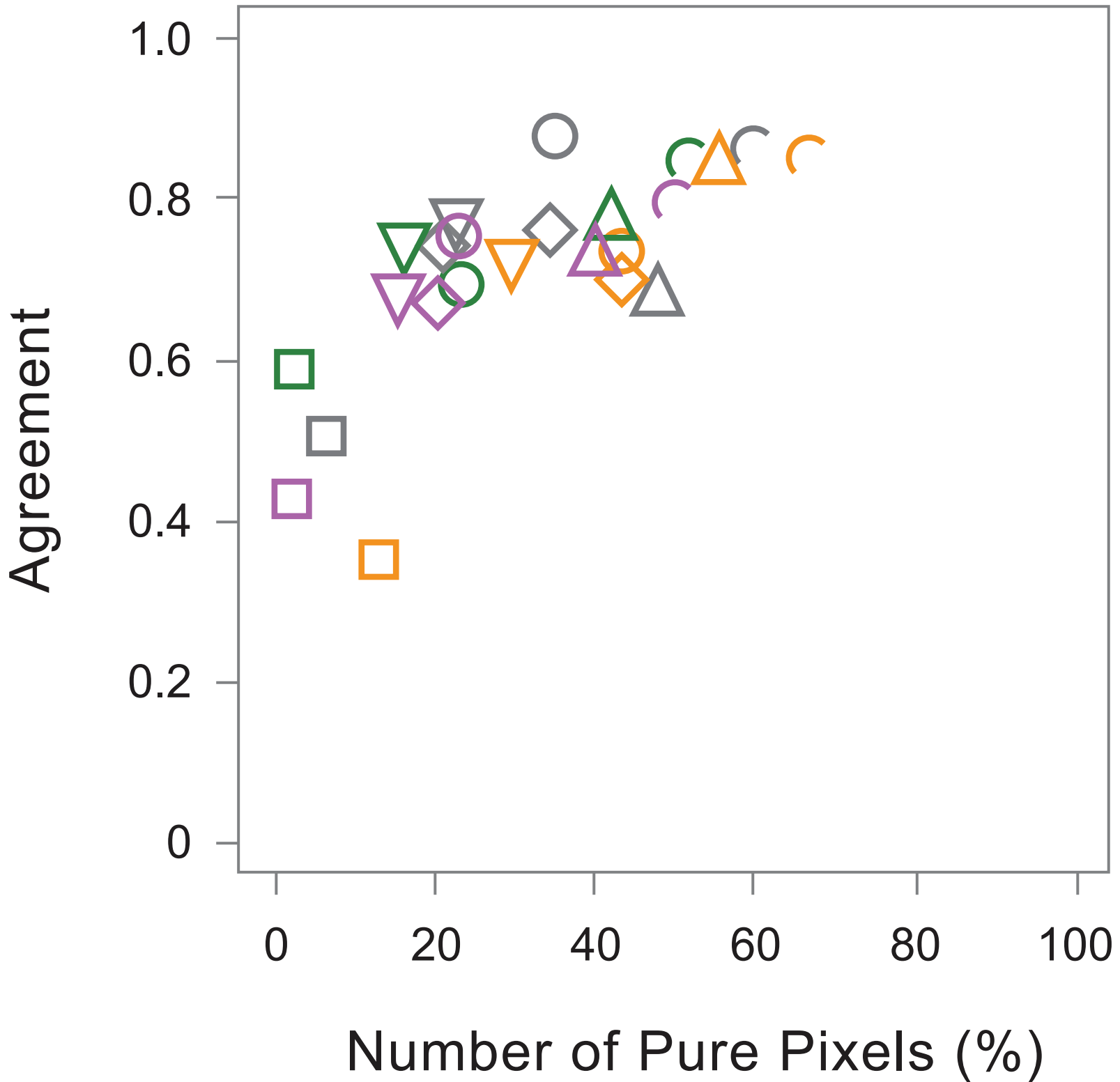


Figure 8 BW (PRINT)

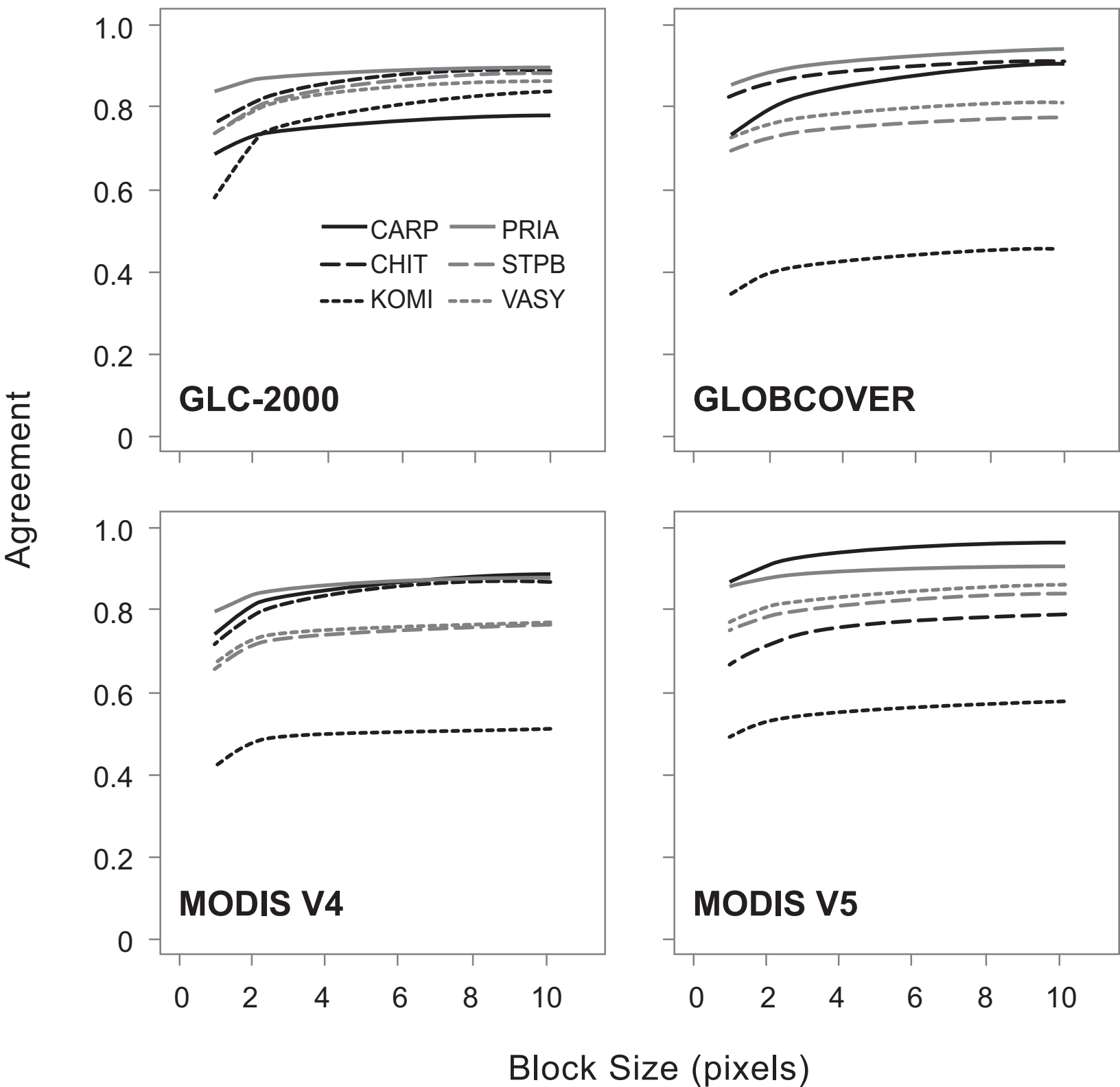


Figure 9 BW (PRINT)

